Journal of Sedimentary Research

Journal of Sedimentary Research, 2018, v. 88, 148–176
Perspectives
DOI: http://dx.doi.org/10.2110/jsr.2017.73

BACK TO BASICS OF SEQUENCE STRATIGRAPHY: EARLY MIOCENE AND MID-CRETACEOUS EXAMPLES FROM THE NEW JERSEY PALEOSHELF

KENNETH G. MILLER, CHRISTOPHER J. LOMBARDI, JAMES V. BROWNING, WILLIAM J. SCHMELZ, GABRIEL GALLEGOS, GREGORY S. MOUNTAIN, AND KIMBERLY E. BALDWIN

Department of Earth and Planetary Sciences and Institute of Earth, Oceans, and Atmospheric Sciences, Rutgers University, Piscataway, New Jersey 08854, U.S.A.

ABSTRACT: **Many sequence stratigraphic approaches have used relative sea-level curves that are dependent on models or preconceived notions to recognize depositional sequences, key stratal surfaces, and systems tracts, leading to contradictory interpretations. Here, we urge following basic sequence stratigraphic principles independent of sea-level curves using seismic terminations, facies successions and stacking patterns from well logs and sections, and chronostratigraphic data to recognize sequence boundaries, other stratal surfaces, parasequences, and systems tracts. We provide examples from the New Jersey siliciclastic paleoshelf from the: 1) early Miocene using academic-based chronostratigraphic, seismic, core, downhole, and core log data, and 2) mid-Cretaceous using commercial well-log, seismic, and biostratigraphic data. We use classic criteria to identify sequence boundaries on seismic profiles by reflection terminations (onlap, downlap, erosional truncation, and toplap), in cores by surfaces of erosion associated with hiatuses detected using biostratigraphy and Sr-isotope stratigraphy and changes in stacking patterns, and in logs by changes in stacking patterns. Maximum flooding surfaces (MFSs) are major seismic downlap surfaces associated with changes from retrogradational to progradational parasequence stacking patterns. Systems tracts are identified by their bounding surfaces and fining- (generally deepening) and coarsening- (generally shallowing) upward trends in cores and well-log stacking patterns. Our Miocene examples of sequences m5.4 (17.7–16.1 Ma) and m5.8 (20.1–19.2 Ma) illustrate how basic sequence stratigraphic techniques reveal higher-order sequences within Myr scale composite sequences. Our mid-Cretaceous examples from the New Jersey shelf provide a paleoshelf transect spanning the Great Stone Dome to the outer continental shelf to identify parasequences, sequences, and systems tracts. This sequence stratigraphic framework provides insights into Myr scale coeval depositional environments across the paleoshelf and reservoir continuity, and highlights the application of basic sequence stratigraphic criteria to reservoir-scale evaluation, not only for oil and gas resources, but also for carbon storage.**

INTRODUCTION

The field of stratigraphy was rejuvenated as one of the pillars of the geosciences by three major advances: the advent of plate tectonics, astronomical times scales, and sequence stratigraphy. The latter was initially developed using seismic profiles (Vail et al. 1977; Mitchum et al. 1977) with the first widely accepted definition of a depositional sequence as a: "stratigraphic unit composed of a relatively conformable succession of genetically related strata and bounded at its top and base by unconformities or their correlative conformities" (Mitchum et al. 1977, p. 53). Sequence stratigraphy was later broadened to integrate outcrop, wells, cores, and downhole logs (Vail 1987; Van Wagoner et al. 1987; Posamentier and Vail 1988; Posamentier et al. 1988). Other important advances included the application of the concept of linked depositional systems called systems tracts to recognize distinct facies successions within sequences (concept of Brown and Fisher 1977 first codified by Vail 1987) and recognition that often the sequence stratigraphic record is composed of parasequences, "... relatively conformable succession of genetically related beds or bedsets bounded by marine flooding surfaces..." (Van Wagoner et al. 1987, p. 11). Parasequences are upward-shallowing successions of facies and are the fundamental components of sequences occurring in all systems tracts (Van Wagoner et al. 1988, 1990). Historical overviews of the development of the field of sequence stratigraphy are provided by Nystuen (1998), Embry (2009), and Donovan (2010). In the following introduction, we highlight primary definitions of sequences, parasequences, stratal surfaces, and systems tracts and objective criteria for their recognition.

One of the great achievements of Vail and colleagues was the recognition of the fundamental nature of unconformities and that sequences are the building blocks of the stratigraphic record. Sequence boundaries are regional surfaces of erosion and/or nondeposition that can be objectively recognized with seismic, outcrop, and chronostratigraphic data. Seismically identified sequence boundaries should be associated not only with downward shifts in onlap, but also distal downlap, erosional truncation, and toplap (Mitchum et al. 1977), ideally traced around a seismic grid to avoid interpreting apparent onlap as true onlap. In outcrops and cores, sequence boundaries can be identified by erosional surfaces with irregular contacts, rip-up clasts, other evidence of reworking, intense bioturbation, major facies changes, stacking-pattern changes (e.g., changes in coarsening versus fining upward), and evidence for hiatuses (Van

Published Online: January 2018
 1527-1404/18/088-148/$03.00

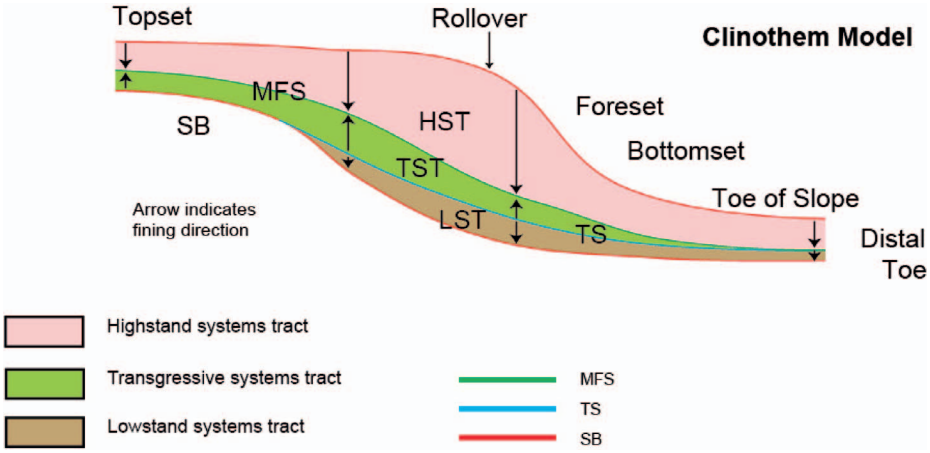

FIG. 1.—Clinothem model used here. Arrows point in fining (deepening) direction. SB, sequence boundary (red lines); TS, transgressive surface (blue lines); MFS, maximum flooding surface (green lines); LST, lowstand systems tract (brown); TST, transgressive systems tract (green); HST, highstand systems tract (light pink). Rollover is equivalent to shelf break and depositional shelf break of authors.

Wagoner et al. 1987; Miller et al. 2013a, 2013b). Sequence boundaries can be identified in well logs by changes in stacking patterns (Van Wagoner et al. 1987; Neal and Abreu 2009), and in marine siliciclastic strata they are commonly associated with low gamma-ray-log values in HST and increases upsection associated with sequences boundaries; in contrast, flooding surfaces (particularly maximum flooding surfaces [MFSs]) are marked by gamma-ray-log increases associated with peak values. In all cases, regional coverage and chronostratigraphic control are needed to demonstrate that sequence boundaries are significant events in a basin.

Much has been made of whether the unconformity that bounds a given sequence is subaerial or submarine (e.g., Plint and Nummendal 2000; Catuneanu et al. 2009); some of these studies restrict sequence boundaries to surfaces with evidence of subaerial unconformities. Unequivocal subaerial criteria are often lacking, especially in cores (e.g., Miller et al. 2013b), and we argue that subaerial exposure is not a requisite criterion for recognizing sequence boundaries. The concept of a sequence boundary is tied not to subaerial exposure, but to regional erosional surfaces that can be traced over large portions of a basin. There are many surfaces of erosion in the geologic record (from local fluvial or marine channels, to transgressive and ravinement surfaces [TSs], to local unconformities of various causes), but ultimately a sequence boundary must be shown to be regional in extent and have a hiatus associated with it.

Sequence stratigraphy is ultimately based on surfaces, including not only sequence boundaries but also MFSs and TSs. The TS marks a change from aggradational or progradational to retrogradational stratigraphic successions on seismic profiles (Neal and Abreu 2009) and a change in cores from coarsening-upward to fining-upward successions (Fig. 1) in siliciclastic shelf depositional environments (though these patterns may be complicated in nearshore settings). The TS may appear as a shift from regressive sands below to finer-grained muds above (Vail 1987; Van Wagoner et al. 1987, 1988, 1990; Posamentier and Vail 1988; Posamentier et al. 1988). The TS can be diachronous along parts of its extent and is commonly linked to local erosion associated with marine ravinement as shoreface erosion cannibalizes former shoreface deposits (Demarest and Kraft 1987).

The maximum flooding surface is "...a downlap surface that is associated with the condensed section..." (Vail 1987 p. 3; see Loutit et al. 1988 for discussion of condensed sections) and a "...surface of deposition at the time the shoreline is at its maximum landward position (i.e. the time of maximum transgression)" (Posamentier and Allen 1999; http://www.sepmstrata.org/page.aspx?pageid=283). The MFS has been advocated as the best means of recognizing a regionally correlatable stratigraphic surface and serves as the cornerstone of "genetic sequences" (Galloway 1989), because it is easily recognizable in multiple types of data. First, in seismic sections the MFS is typically a downlap surface (DLS; usually the lowest marine DLS in the topset region of a depositional sequence where multiple DLSs occur; Miller et al. 2013b); second, it is often represented by an upsection change from retrogradational to progradational successions in seismic profiles, outcrops, cores, and well logs (Neal and Abreu 2009); and third, in marine siliciclastic sections (cores and outcrops) it corresponds to a change from fining-upward to coarsening-upward successions (Fig. 1; Vail 1987; Van Wagoner et al. 1987, 1988; Posamentier and Vail 1988; Posamentier et al. 1988). The deepest paleowater depth of a sequence is often associated with the MFS in condensed sections with high degrees of bioturbation, *in situ* glauconite, phosphorite, organic carbon, mud peaks, the highest percentage planktonic foraminifera (and other plankton or nekton), and *in situ* shells (Loutit et al. 1988; Kidwell 1989, 1991).

System tracts are linked contemporaneous depositional systems that can be recognized by both their facies successions and their bounding surfaces (Brown and Fisher 1977). Sequences are generally subdivided into LST, TST, and HST (Vail 1987; Van Wagoner et al. 1987; Posamentier and Vail 1988; Posamentier et al. 1988). In addition a falling-stage systems tract (FSST) is often recognized (Posamentier et al. 1992; Plint and Nummendal 2000). The LST, TST, and HST are separated by two distinct stratal surfaces, the TS and the MFS (Fig. 1). LSTs lie directly on the sequence boundary, are the lower regressive systems tract, contain progradational to aggradational parasequence sets, and generally shallow and coarsen up to the TS (Fig. 1; Vail 1987; Van Wagoner et al. 1987; Posamentier et al. 1988; Coe 2003; Neal and Abreu 2009). The TS generally separates the LST below from the TST above. Where no LST deposits are present or in seismic data where thin LST sediments are below seismic resolution, the TS merges with the sequence boundary (Fig. 1). The TST is transgressive and contains generally fining-upward parasequences (Fig. 1); though individual parasequences may coarsen and shallow upsection with the TST, the overall systems tract contains retrogradational facies. The MFS separates the TST and the HST. The HST is regressive, downlaps onto the MFS, and is generally overlain by the upper sequence boundary (Vail 1987; Van Wagoner et al. 1987, 1988; Posamentier and Vail 1988; Posamentier et al. 1988). The HST is associated with progradational to aggradational parasequence sets (Neal and Abreu 2009). Some workers use the term FSST for the degradational parasequence set where facies on top of the HST gradually step down ("forced regression," Posamentier and Allen 1999; Plint and Nummendal 2000; Hunt and Tucker 1992; Catuneanu 2002). We do not use the FSST here, but we review its possible applications and complications in the Discussion.

The criteria for recognizing sequences and systems tracts based on geometry, stacking pattern (retrogradational, progradational, aggradational), and facies successions (either fining or coarsening upward in the siliciclastic example) are objective, but the interpretations of sequences are often tied to genetic criteria (Mitchum et al. 1977), especially changes in

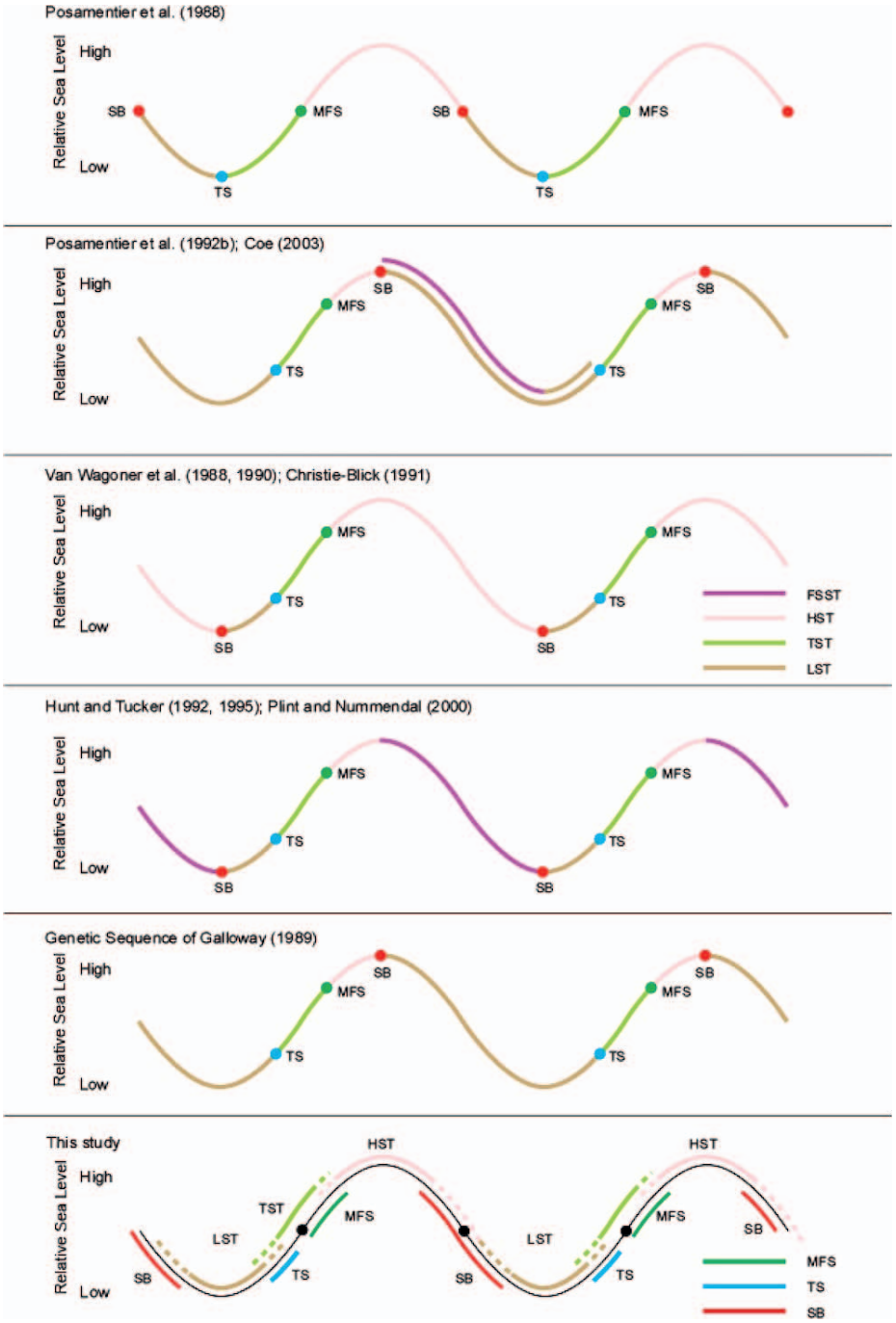

FIG. 2.—Comparison of conceptual sea-level models. See Figure 1 caption for definition of terms.

relative sea level. Relative sea level is a debatable term, but it was originally defined as "...an apparent rise or fall of sea level with respect to the land surface"... (Mitchum 1977, p. 209) or "...the position of the sea surface with respect to the position of a datum (e.g., basement)..." (Posamentier et al. 1988, p. 110). Whereas there are notable exceptions (e.g., Embry 2009), most sequence stratigraphic methodologies (e.g., Posamentier et al. 1988; Coe 2003; Catuneanu et al. 2009; http://www.sepmstrata.org/page.aspx?&pageid=32&3) tie systems tracts to a hypothetical relative or eustatic (global mean) sea-level curve (Fig. 2; also see summary in Catuneanu et al. 2009) and definitions of systems tracts seem inseparable from sea level (e.g., Coe 2003).

Early conceptual sequence stratigraphic models interpreted deposition of: 1) the LST from the time of maximum rate of relative or eustatic fall associated with the sequence boundary to the beginning of the rise (Fig. 2; Pitman and Golevchenko 1983; Posamentier et al. 1988); 2) the TST from the beginning of the rise to the time of the maximum rate of rise at the MFS (Fig. 1; Galloway 1989); and 3) the HST from the maximum rate of rise to the time of maximum rate of fall (Fig. 2; Posamentier and Vail 1988). Subsequent publications have developed strikingly different timings (e.g., with the LST lagging more than one-quarter cycle and starting at the beginning of the rise and the MFS late in the relative rise) of systems tracts with respect to hypothetical sea-level curves (Fig. 2; e.g., Coe 2003;

Catuneanu et al. 2009). We illustrate (Fig. 2) numerous conceptual models and their multiplicity and non-uniqueness of interpretations. Use of sea level in the definitions is entirely dependent on models or preconceived notions; thus, we strongly advocate against linking sequence boundaries, MFSs, TSs, and systems tracts to any specific point of relative sea level. Application of *any* model is an oversimplification because position of a stratal surface with respect to changes in relative sea-level is a function of pre-existing geometry, rates of subsidence (including differential subsidence that precludes computation of a single relative sea-level curve), and sediment supply (including shifting depocenters; e.g., Christie-Blick et al. 1990). In a sense, all models (Fig. 2) are correct in certain settings and are incorrect in general. We illustrate this with our conceptual model that incorporates most previous models and shows surfaces and systems tracts associated with zones on an idealized relative change in sea level, but invalidates attempts to uniquely relate stratal surfaces and systems tracts to a specific point on a curve of relative sea level (Fig. 2).

Sequence stratigraphic approaches have become increasingly divergent as researchers have used strikingly different definitions of systems tracts with respect to sea level and sequence nomenclature (e.g., Fig. 2; Catuneanu 2002; Catuneanu et al. 2009). This led some to plea for a return to basics (Neal and Abreu 2009), an approach we adopt here. In his definition, Mitchum et al. (1977, p. 53) said it best: "A depositional sequence is determined by a single objective criterion, the physical relations of the strata themselves. The combination of objective determination of sequence boundaries and the systematic patterns of deposition of the genetically related strata within sequences makes the sequence concept a fundamental and extremely practical basis for the interpretation of stratigraphy and depositional facies."

Neal and Abreu (2009) and Miller et al. (2013b) focused on the basic stratal surfaces (SB, TS, and MFS) and stacking patterns of parasequence sets to interpret sequences, eschewing the use of changes in relative sea level in recognizing systems tracts. Neal and Abreu (2009) emphasized the use of stacking within sequences, including progradational–aggradational–retrogradational–degradational patterns observed in seismic profiles. Miller et al. (2013b) also adopted a "back to basics" approach to New Jersey Miocene sequences (Fig. 1) drilled by Expedition 313, applying stacking patterns in cores and logs to decipher systems tracts.

Here, we revisit New Jersey early Miocene sequences and provide new data for the mid-Cretaceous of the New Jersey paleoshelf to illustrate our back-to-basics approach. We show that integrating reflection terminations, core and log stacking patterns, grain-size changes, and chronostratigraphic control provides strong constraints on systems tracts that would be ambiguous and often inconsistent if based on preconceived notions and relative sea-level curves. We do not tie our interpretations to changes in relative sea level. Rather, we simply use seismic, core, and well log stacking patterns to define sequence boundaries, MFS, TS, and facies successions within sequences. In turn, we use facies successions and stratal surfaces to subdivide sequences into systems tracts. We suggest that surfaces and system tracts fall within broad windows of potential sea-level curves and are not anchored to any specific position (Fig. 2). Our approach is hardly novel, but it does illustrate that although sequence stratigraphy as a practicing science has become unnecessarily complicated, it can be simplified to an objective and useful approach.

BACKGROUND AND METHODS

The Mid-Atlantic U.S. Margin

The Mid-Atlantic U.S. passive continental margin (Figs. 3, 4) contains thick (2–16 km) post-rift (upper Lower Jurassic and younger) sediments in the offshore Baltimore Canyon Trough (BCT) basin and thinner (0–2.4 km) uppermost Jurassic to Holocene sediment in the onshore coastal plain in the Salisbury Embayment (e.g., Grow and Sheridan 1988). Rifting occurred during the Late Triassic to earliest Jurassic (230–198 Ma) followed by extrusion of Early Jurassic seaward-dipping basalts (Talwani et al. 1995). Seafloor spreading began before the Callovian ($\sim$ 165 Ma; Middle Jurassic; e.g., Grow and Sheridan 1988), with the likely opening beginning off Georgia ca. 200 Ma and progressing northward off the Mid-Atlantic margin by ca. 180 Ma (Withjack et al. 1998). This south-to-north "zipper" onset of seafloor spreading is associated with a diachronous post-rift unconformity that separates active "rift-stage" deposits from more passive-margin "drift-stage" deposits that accumulated in an ever-widening and deepening basin open to the ocean. Post-rift history was generally dominated by passive simple thermoflexural subsidence and loading (Steckler and Watts 1978; Grow and Sheridan 1988; Kominz et al. 1998, 2002). Subsidence began offshore in the Early Jurassic and progressively moved onshore from the Late Jurassic to the Early Cretaceous (ca. 150 to 125 Ma) as a thermoflexural response to increasing crustal rigidity (Watts 1981; Grow and Sheridan 1988; Olsson et al. 1988). The region has provided an excellent record of changes in relative sea level (e.g., Olsson et al. 1987; Miller et al. 2005), though glacial isostatic adjustments (GIAs) complicate the Pliocene and younger record (e.g., Peltier 1998; Raymo et al. 2011) and deposition has been impacted by changes in mantle-based dynamic topography (Moucha et al. 2008; Rowley et al. 2011).

The paleophysiography of the Mid-Atlantic U.S. passive continental margin has evolved, causing not only local variations, but also confusion about the definition of the terms shelf, shelf break, and slope. The terms shelf, slope, and rise were first defined based on physiographic observations on the U.S. middle Atlantic margin on the basis of seafloor gradient and subsequently applied globally: the continental shelf dips seaward with a gradient of less than 1:1000 ($< 0.06°$), the continental slope with a gradient greater than 1:40 ($> 1.4°$), and the continental rise with a gradient of about 1:100 ($\sim 0.6°$; Heezen et al. 1959; Emery 1968). The continental shelf is wide (> 150 km) in this region and the water depth at the shelf break averages about 135 m (Heezen et al. 1959), ranging from 80 to 200 m (Goff et al. 2013). The modern physiographic terms shelf, slope, and rise are not directly related to the paleo-margin because the U.S. middle Atlantic margin evolved from a carbonate ramp to a prograding siliciclastic margin during the Eocene to Miocene (Steckler et al. 1999; Miller et al. 2013a), and paleogeomorphology of the Cretaceous has not been reconstructed. The change in margin morphology is revealed by reconstruction of past depositional surfaces using two-dimensional back-stripping for the Cenozoic (Steckler et al. 1999). Whereas the structural shelf break has remained > 100 km offshore, prograding clinothems (Fig. 1; prograding units bounded by seismic unconformities) are buried beneath the inner (early Miocene; Fig. 5), middle (middle Miocene), and outer continental shelf (late Neogene), with clinoform rollovers deposited on a shallow shelf ($\sim$ 20–100 m). Only during the Pleistocene did the clinothems prograde sufficiently far that the clinoform rollovers were near the modern structural shelf break. Thus, we eschew the use of the modern terms shelf, slope, and rise for paleophysiography since they have a preferred paleodepth connotation and generally are associated with the geological boundary between thinned continental crust and oceanic crust. The geometry of buried clinothems beneath the present-day shelf consists of topset, foreset, and bottomset beds. The change in declivity between the topset and foreset has been termed shelf edge (Vail and Todd 1981), shelf break, depositional coastal or shoreline break (Vail 1987; Van Wagoner et al. 1987), seafloor break (Donovan 2010), and clinoform rollover (Fig. 1); we prefer the geometric term *clinoform rollover* due to its descriptive nature (Fig. 1). As noted here and elsewhere (Van Wagoner et al. 1987; Donovan 2010; Miller et al. 2014), the clinoform rollover may be many hundreds of kilometers landward of the structural shelf break. We thus use the geometric terms topset, clinoform rollover, foreset, and bottomset (Fig. 1) to describe the paleophysiography of the paleoshelf, as observed on many margins throughout the world (Bartek et al. 1991).

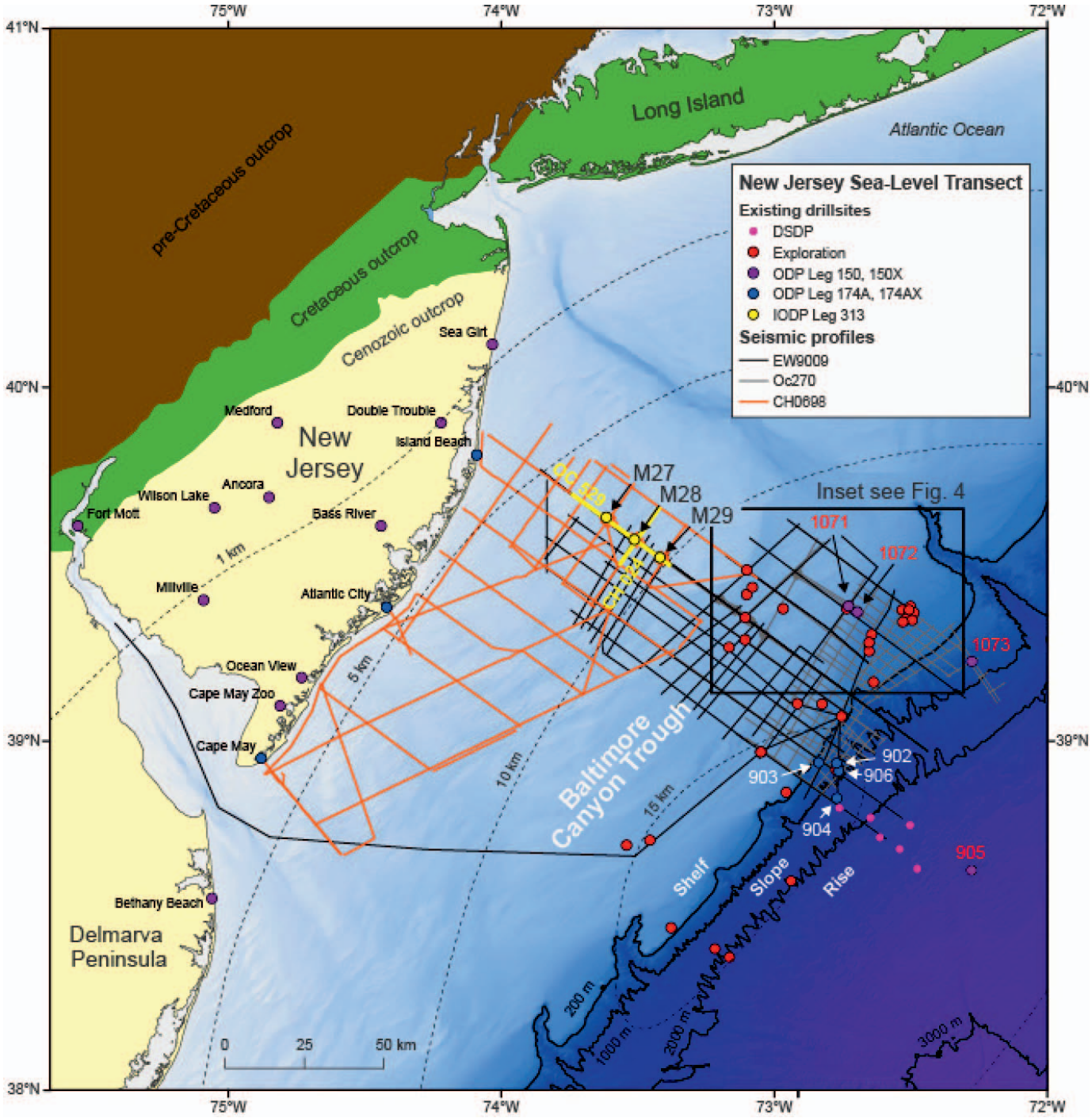

FIG. 3.—Shaded generalized bathymetric location map of the New Jersey and Mid-Atlantic Margin sea-level transect showing three generations of MCS data (cruises *Ew9009*, *Oc270*, and *Ch0698*), onshore coreholes, and offshore coreholes drilled by ODP, IODP, and industry. Dashed lines indicate structural contours on depth to basement and outline the Baltimore Canyon Trough. Black box outlines area shown in Figure 4.

Academic Multichannel Seismic Imaging, Coring, and Logging

Two seismic and two drilling campaigns targeted the BCT and onshore coastal-plain region, one by industry (1975–1983) and one by scientific ocean drilling (1983–2009). Several seismic grids obtained on the New Jersey continental shelf and slope (Fig. 3) targeted Miocene and younger strata first imaged by industry data (Greenlee et al. 1992) and aided the planning of academic drilling by Ocean Drilling Program (ODP) Leg 150 on the continental slope (Mountain et al. 1994), Leg 174A on the outmost shelf and slope (Austin et al. 1998), and the Integrated Ocean Drilling Program (IODP) Expedition 313 on the inner–middle continental shelf (Mountain et al. 2010). A reconnaissance grid was shot by R/V *Ewing* cruise *Ew9009* (Fig. 3) in 1990 across the shelf and slope using a 120-channel, six-air-gun system with ~ 10 m vertical resolution. This was followed by: 1) a higher-resolution, mid–outer shelf grid shot by the R/V

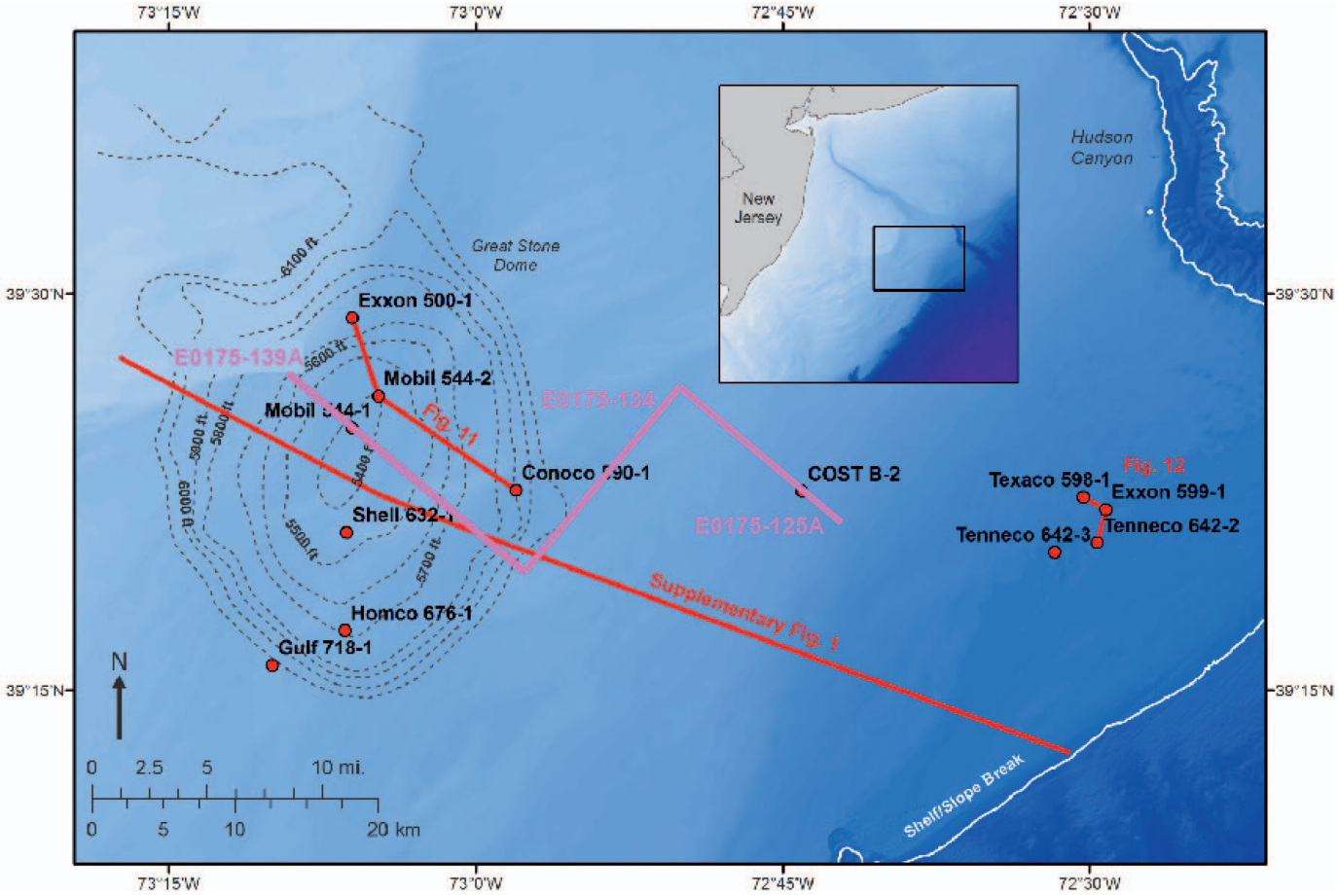

FIG. 4.—Shaded generalized bathymetric location map of the Great Stone Dome (structural contours to basement after Prather 1991) and the 12 exploration wells discussed here and shown in Figures 11, 12, and Supplemental Figure S2. Well-log cross sections are shown in red and seismic profiles (Fig. 9) are shown in magenta.

Oceanus cruise *Oc270* in 1995 using a single generator-injector (GI) gun and 48-channel HiRes equipment that provided ~ 5 m vertical resolution; and 2) a nearshore grid by R/V *Cape Hatteras* cruise *CH0698* using an identical HiRes system. Together, the 2D data collected by *Oc270* and *CH0698* significantly increased the number of resolvable Miocene sequences (Fig. 5A, B) compared with the earlier industry (Greenlee et al. 1992) and *Ew9009* data.

Several studies interpreted the sequence stratigraphy of lower to middle Miocene seismic profiles. Analysis of *Oc270* and *CH0698* seismic profiles (Monteverde et al. 2008; Monteverde 2008) built on earlier analyses by Exxon (Greenlee et al. 1992) and *Ew9009* profiles (Miller and Mountain 1994) by identifying seismic sequence boundaries based on reflection terminations of onlap, downlap, erosional truncation, and toplap. Seismic sequence boundaries from the older datasets were traced and loop correlated throughout the seismic grids (Monteverde et al. 2008; Monteverde 2008). Sequence boundaries can be objectively defined by these terminations, as shown in Figure 5A where terminations (highlighted with red arrows) can be used to pick sequence boundaries (Fig. 5B). In this contribution, we focus on strata between reflections identified as sequence boundaries m6 and m5 that bracket a series of lower to middle Miocene (Aquitanian to Serravalian) sequences continuously cored and logged at Sites M27, M28, and M29 (Figs. 3, 5A, B; Monteverde et al. 2008; Monteverde 2008; Mountain et al. 2010). Sequences are named according to their basal reflection boundary (e.g., sequence m5.4 lies on reflection m5.4; Figs. 5, 6), with numbers increasing down section (e.g., m5.4 lies beneath m5.3).

Continuous coring and logging integrated with core–log–seismic data provided additional constraints on lower to middle Miocene sequences on the New Jersey shallow shelf (Figs. 6–8; Mountain et al. 2010). Expedition 313 Sites M27, M28, and M29 were drilled on *Oc270* Line 529 (Fig. 5A, B). Miocene sequences (ca. 23–13 Ma) were sampled across several unconformity-bounded clinothems at topset, foreset, and bottomset locations. Expedition 313 studies independently recognized sequence boundaries and flooding surfaces in the cores and logs based on integrated study of key core surfaces, lithostratigraphy (grain size, mineralogy, facies, and paleoenvironments), facies successions, benthic foraminiferal water depths, downhole logs, core gamma-ray logs, and chronostratigraphic ages (Mountain et al. 2010; Browning et al. 2013; Miller et al. 2013a). A preliminary velocity–depth function developed from stacking velocities, limited downhole sonic logs, and vertical seismic profiles yielded uncertainties of reflection correlation of ~ ± 5 m (Mountain and Monteverde 2012); comparison of predicted sequence boundaries with major core surfaces, downhole and core logs, and synthetic seismograms, yielded core–seismic–log correlations to better than ± 3 m (Miller et al. 2013a). This procedure showed that Miocene core sequence boundaries correspond remarkably well with acoustic-impedance contrasts, as did other seismic stratal surfaces, particularly maximum flooding surfaces (Miller et al. 2013a). Previous ocean drilling studies have tested and confirmed this tenet of sequence stratigraphy on the Bahamas carbonate platform (Eberli et al. 2002) and the New Jersey slope (Miller et al. 1998), but Expedition 313 was the first to demonstrate this across numerous stratal surfaces on a siliciclastic depth transect of a paleoshelf.

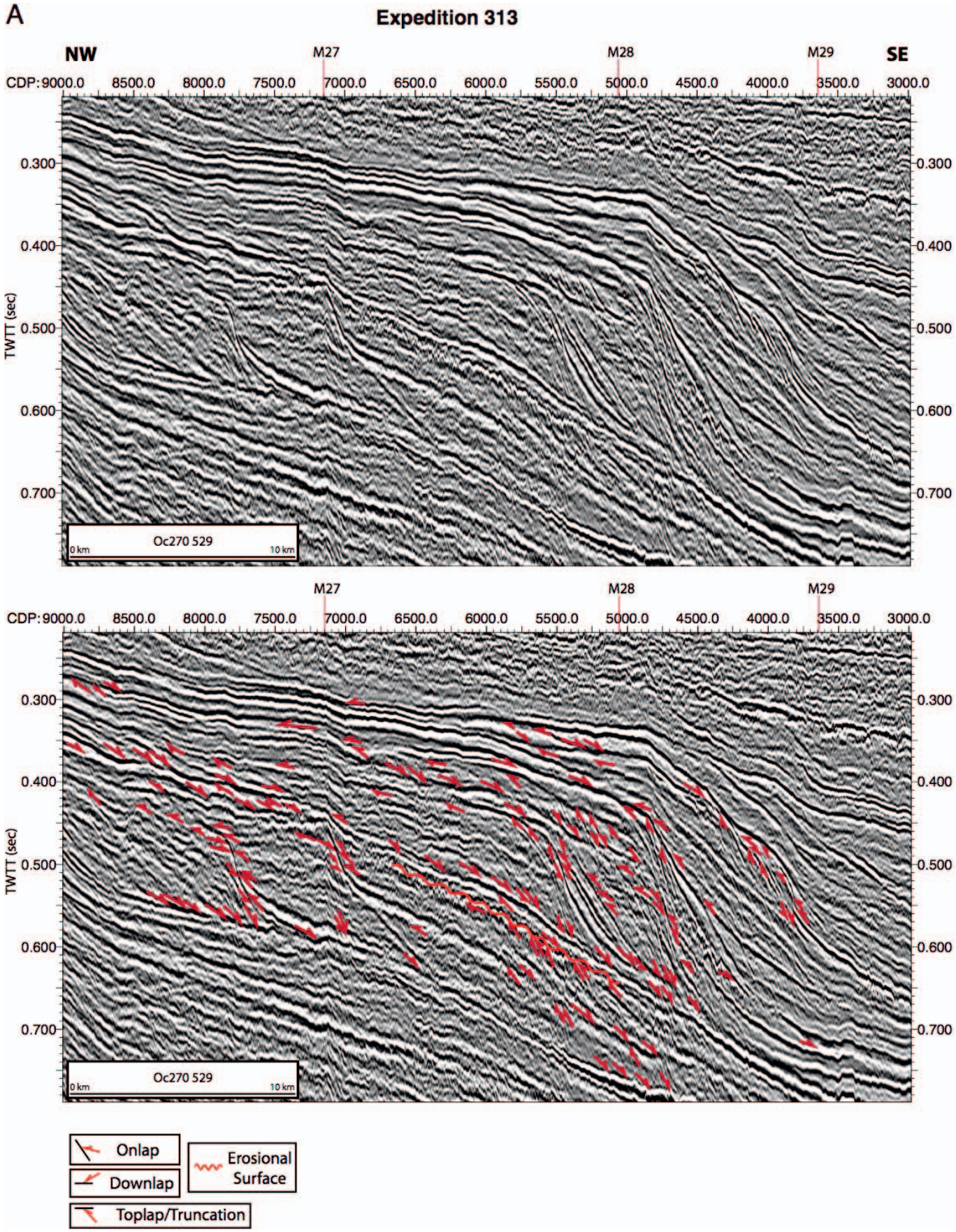

FIG. 5A.—*Oceanus* dip Line 529 uninterpreted (top) and interpreted (bottom) with red arrows indicating onlaps, downlaps, erosional truncations, and toplaps. Wavy line is a mass wasting unconformity.

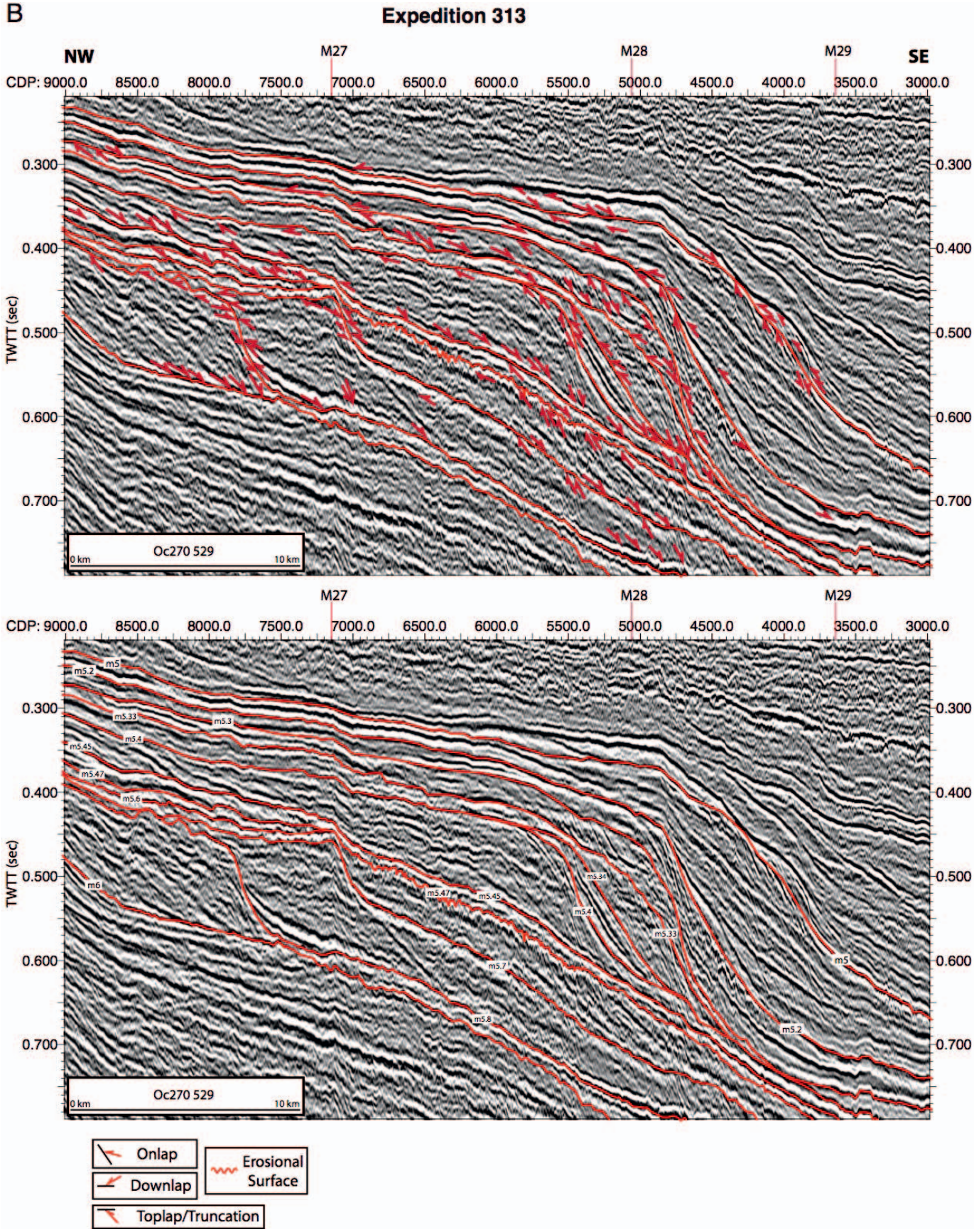

FIG. 5B.—*Oceanus* dip Line 529 and interpreted with sequence boundaries and red arrows indicating onlaps, downlaps, erosional truncations, and toplaps (top panel) and sequence boundaries alone (bottom panel). Wavy line is a mass-wasting unconformity.

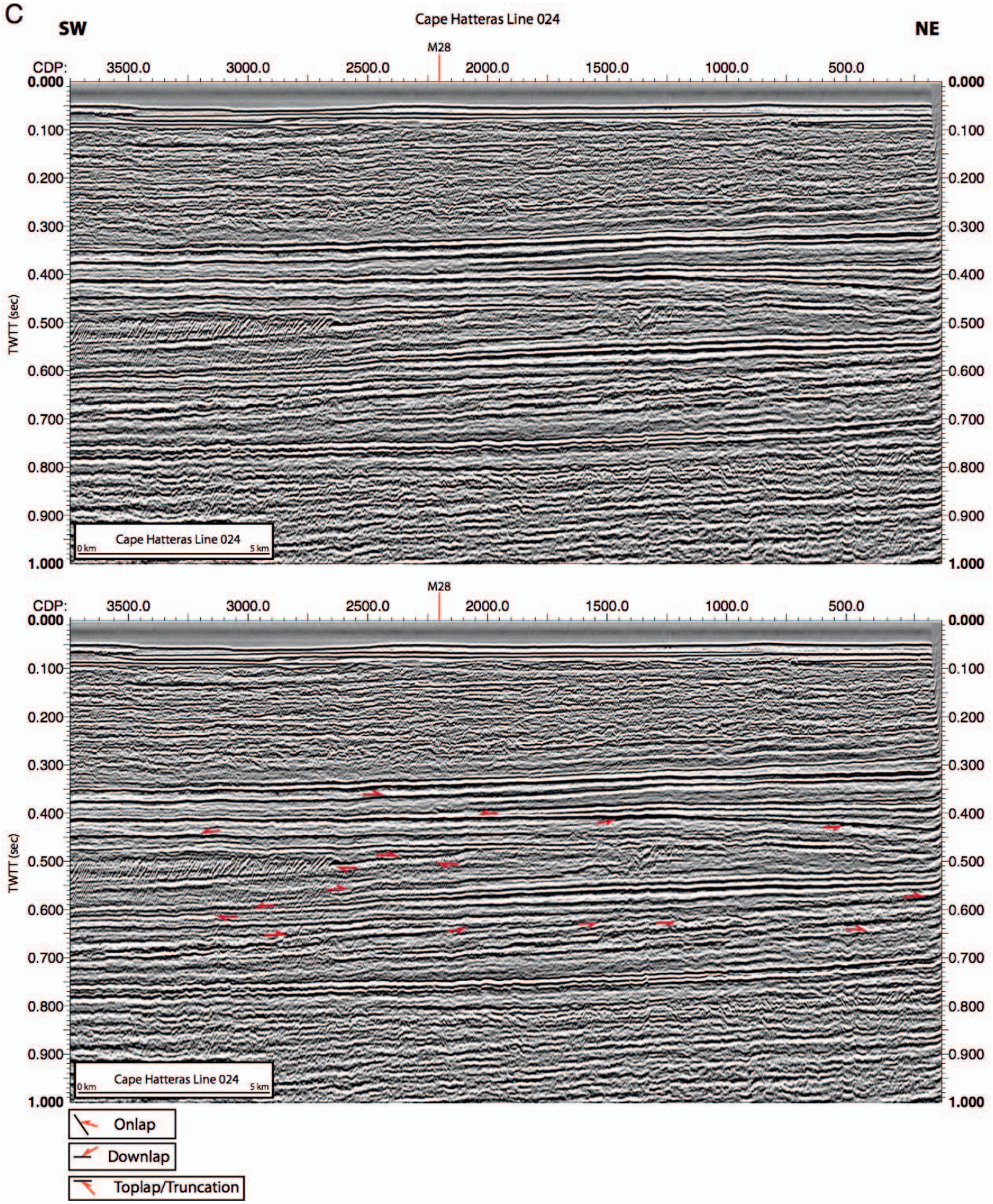

FIG. 5C.—*Oceanus* strike Line 24 uninterpreted (top) and interpreted (bottom) with red arrows indicating onlaps, downlaps, erosional truncations, and toplaps.

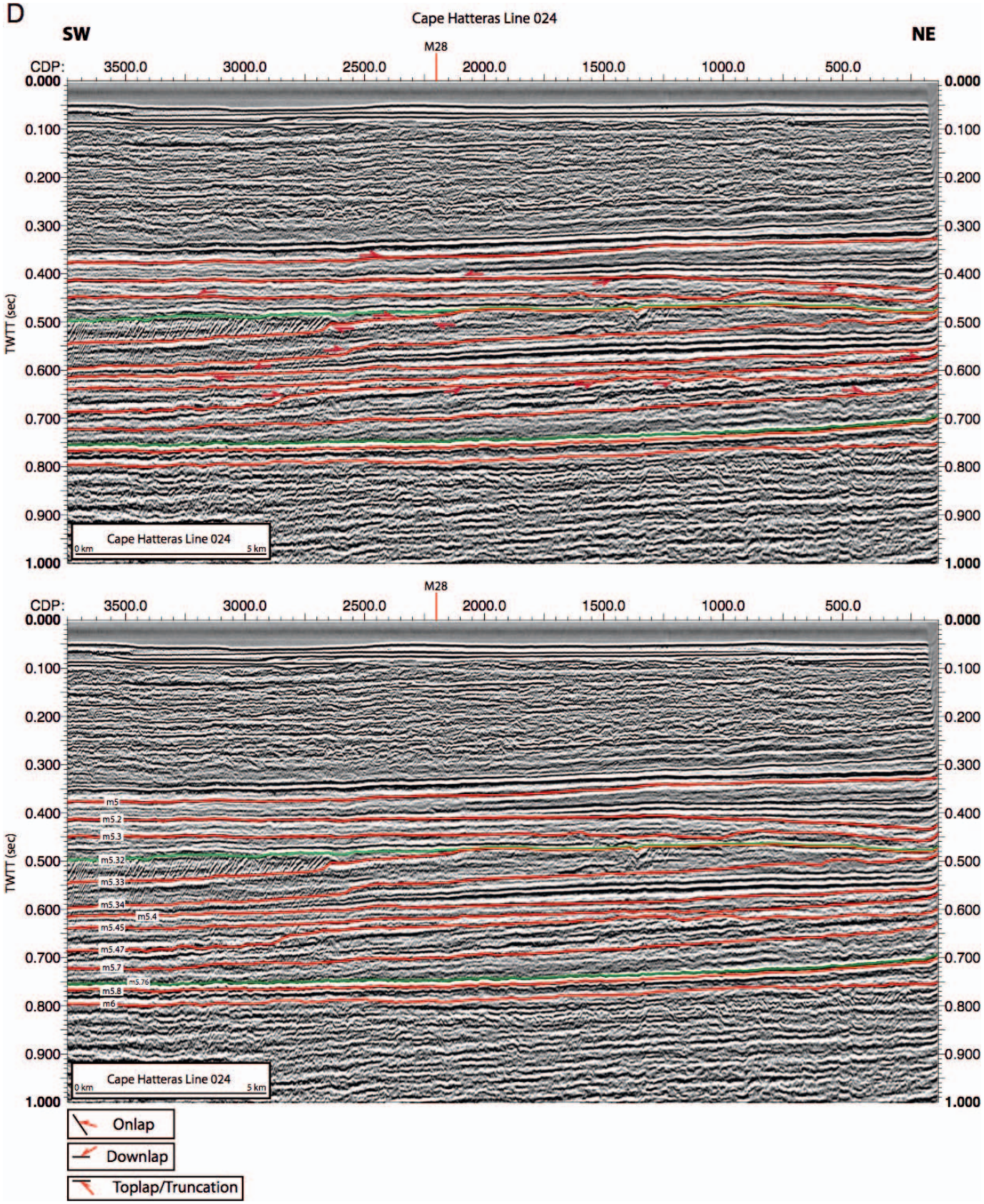

FIG. 5D.—*Oceanus* strike Line 24 interpreted with sequence boundaries and red arrows indicating onlaps, downlaps, erosional truncations, and toplaps (top panel) and sequence boundaries alone (bottom panel).

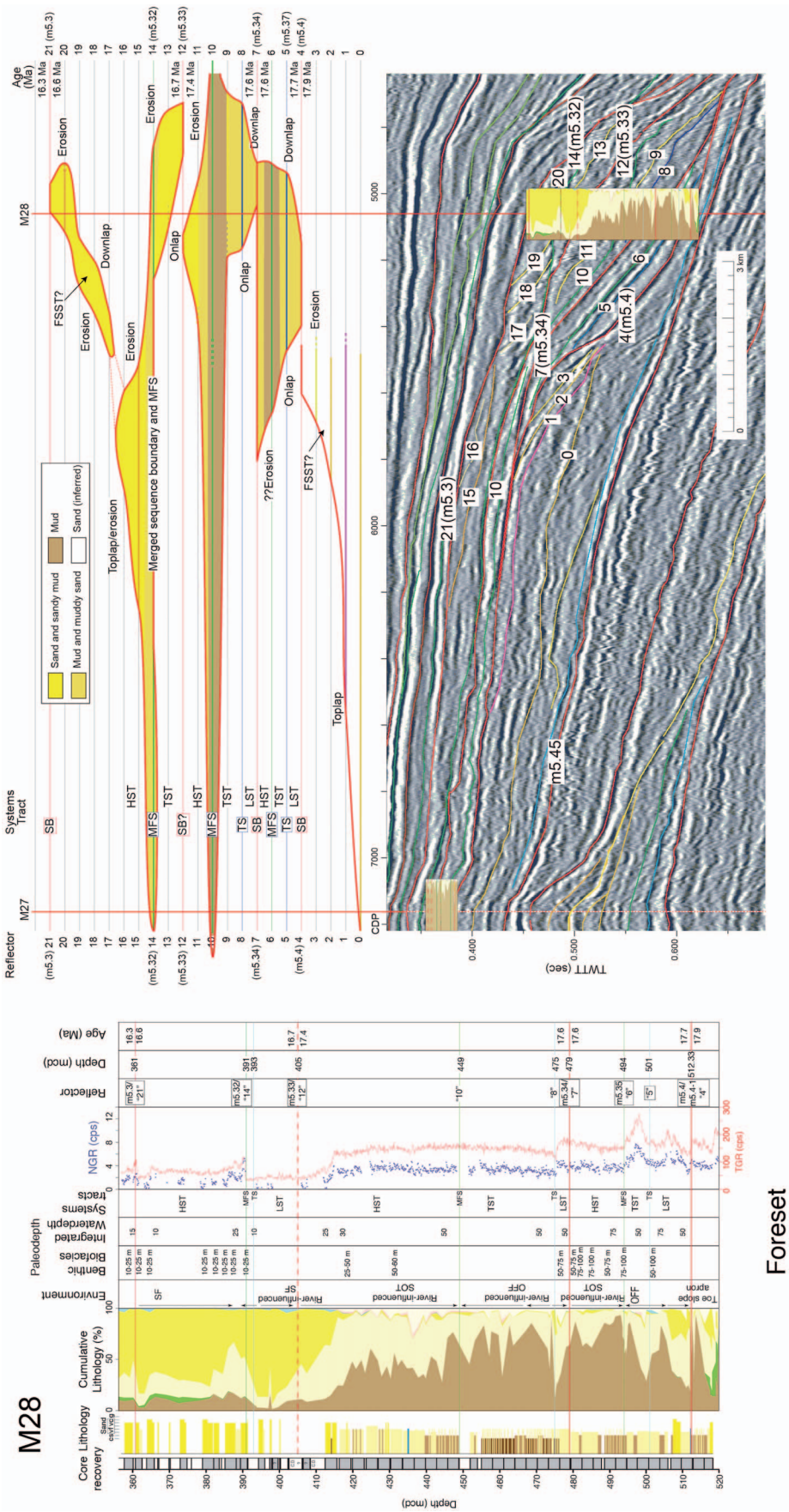

Foreset

FIG. 6.—Left Panel. Sequence m5.4 figures are modified from Miller et al. (2013b). Left panel: Site M28 core showing: core depths in meters composite depth (mcd), core recovery (gray, recovered; white, gap); lithology; c, clay; s, silt; vf, very fine sand; m, medium sand; vc, very coarse sand; g, gravel; coarse fraction cumulative percent lithology (brown, mud; light yellow, fine quartz sand; dark yellow, medium-coarse quartz sand; green, glauconite sand; blue, carbonate [shells and foraminifera]; arrows point in fining direction); symbols on key at upper right; environmental interpretation based on lithofacies after Mountain et al. (2010) (SF, shoreface; SOT, shoreface–offshore transition, lower shoreface; OFF, offshore); paleowater depths in meters based on benthic foraminiferal biofacies after Katz et al. (2013); integrated paleowater depth in meters based on benthic foraminiferal biofacies and lithofacies after Miller et al. (2013a); gamma logs (red, downhole wireline measurements as total gamma ray (TGR) in counts per second (cps), blue dots, natural gamma ray [NGR] measurements made on unsplit whole cores, scale in CPS); data after Mountain et al. (2010); reflections (red, sequence boundary; blue, transgressive surface [TS]; green, maximum flooding surface [MFS]); dashed red lines, uncertain placement of sequence boundary; systems tracts, LST, lowstand systems tract; TST, transgressive systems tract; HST, highstand systems tract, falling stage systems tract. Ages for surface immediately below and above sequence boundaries after Browning et al. (2013).FIG. 6.—Right Panel. Interpreted seismic profile and Wheeler diagram (stratigraphic position vs. distance; Wheeler 1958) of sequence m5.4 across the foreset at Site M28. Bottom panel is interpreted seismic profile in two-way travel time (TWTT) in seconds versus CDP (approximate scale in km given on lower left); red arrows indicate reflection terminations; reflections in red indicate sequence boundaries, blue indicate TS, and green indicate MFS. Other internal reflections are indicated in shades of yellow. Cumulative lithology is superimposed on the site. Arbitrary numbers assigned to reflections are used to construct a time–distance plot at the top; the left-hand scale of the Wheeler diagram assumes constant ages between reflections; age estimates shown in Ma are derived from Browning et al. (2013).

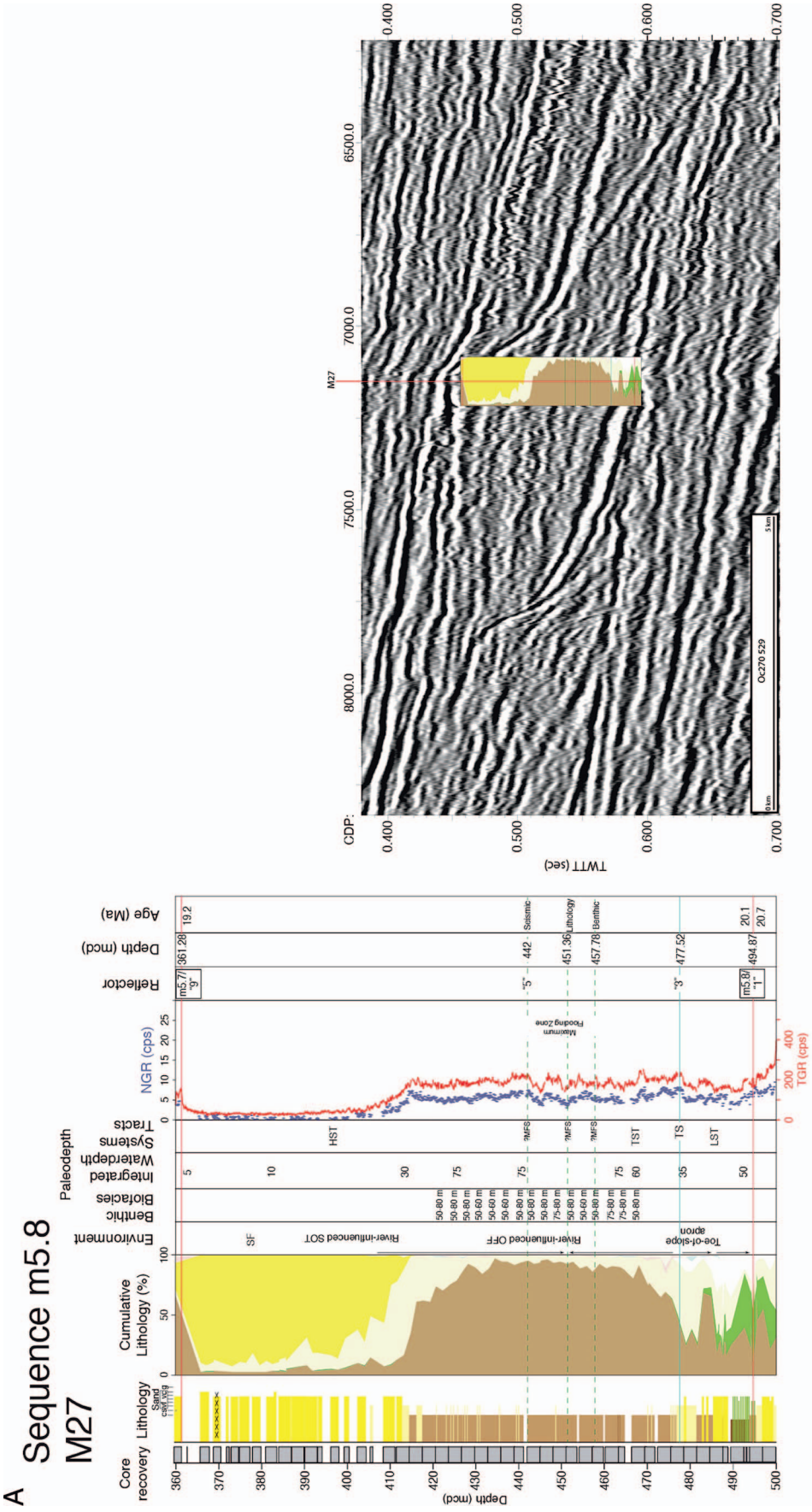

FIG. 7A.—Uninterpreted seismic profiles and stratigraphic section from sequence m5.8 at Site M27. See Figure 6A for key.

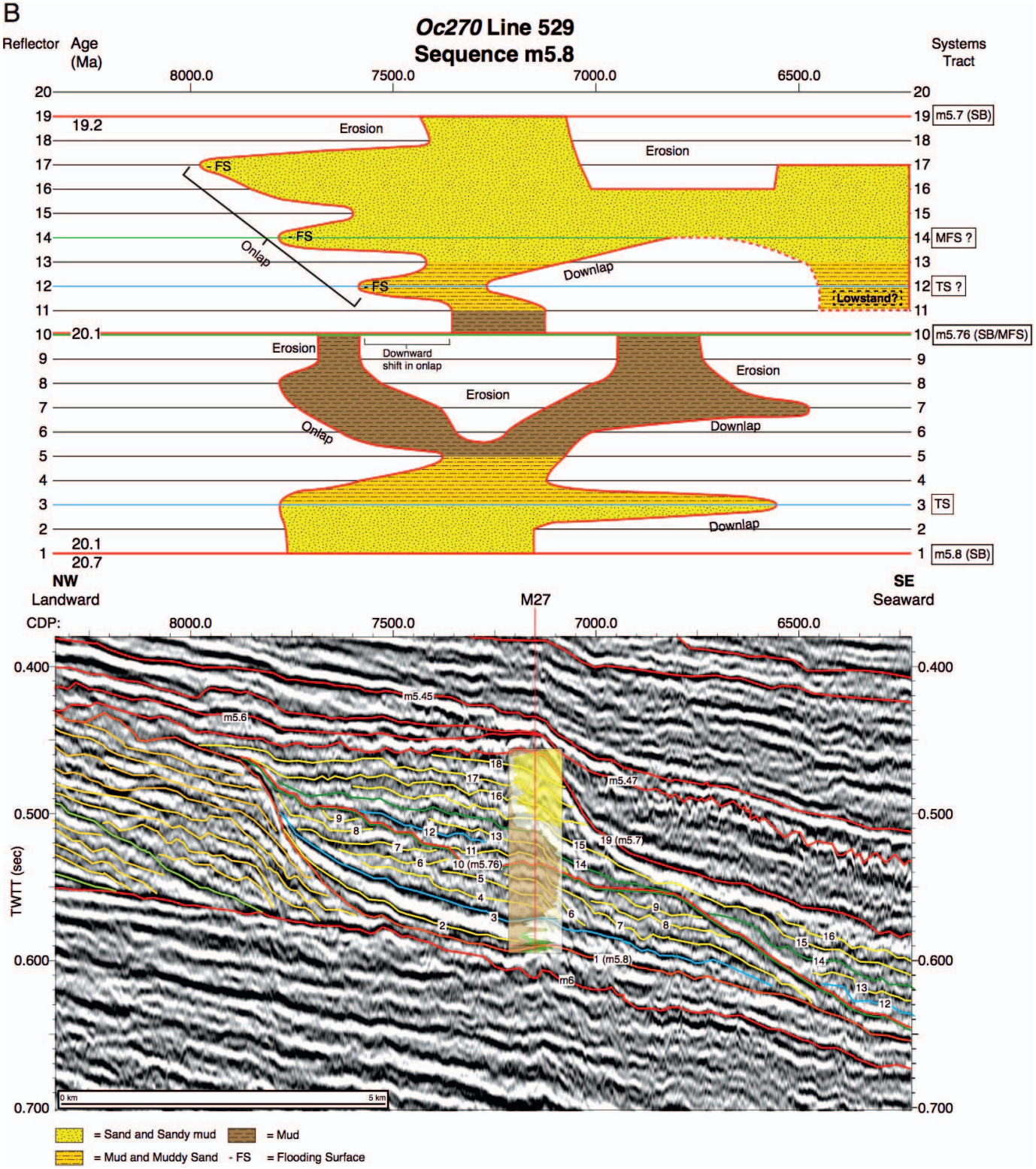

FIG. 7B.—Sequence m5.8 preferred interpretation. See Figure 6 right panel for caption.

Sampling of thick foresets on three sequences (m5.8, m5.4, and m5.2) by Expedition 313 along a transect of seismic clinothems (prograding sigmoidal sequences) allowed Miller et al. (2013b) to test sequence stratigraphic models. They found that landward of the clinoform rollover (Fig. 1), topsets consist of nearshore deposits above merged TS and SB overlain by deepening and fining-upward TST and coarsening and shallowing upward HST. Drilling through the foresets yields thin LST (< 18 m thick), thin TST (< 18 m), and thick HST (15–90 m), contrasting

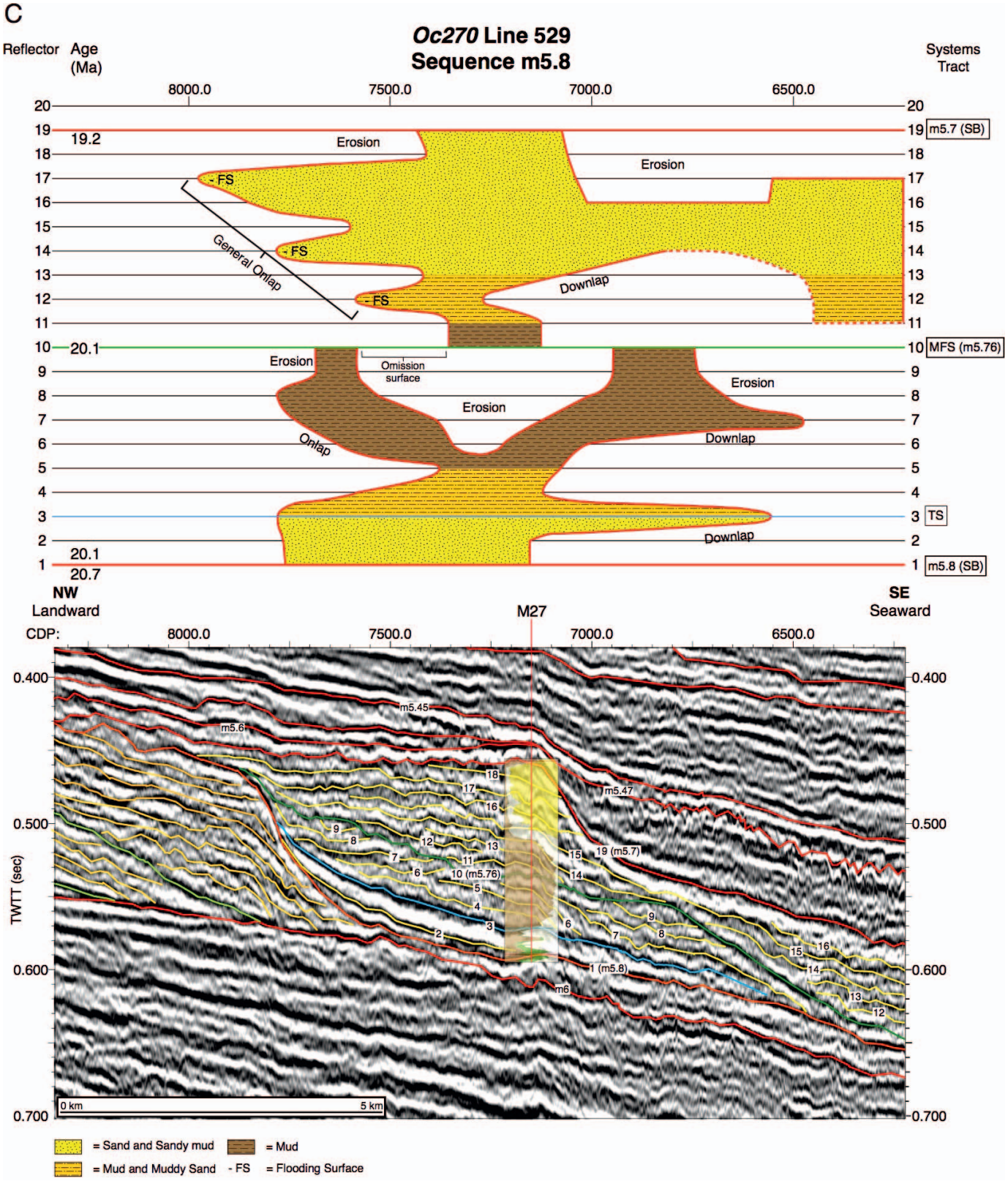

FIG. 7C.—Sequence m5.8 alternate interpretation. See Figure 6 right panel for caption.

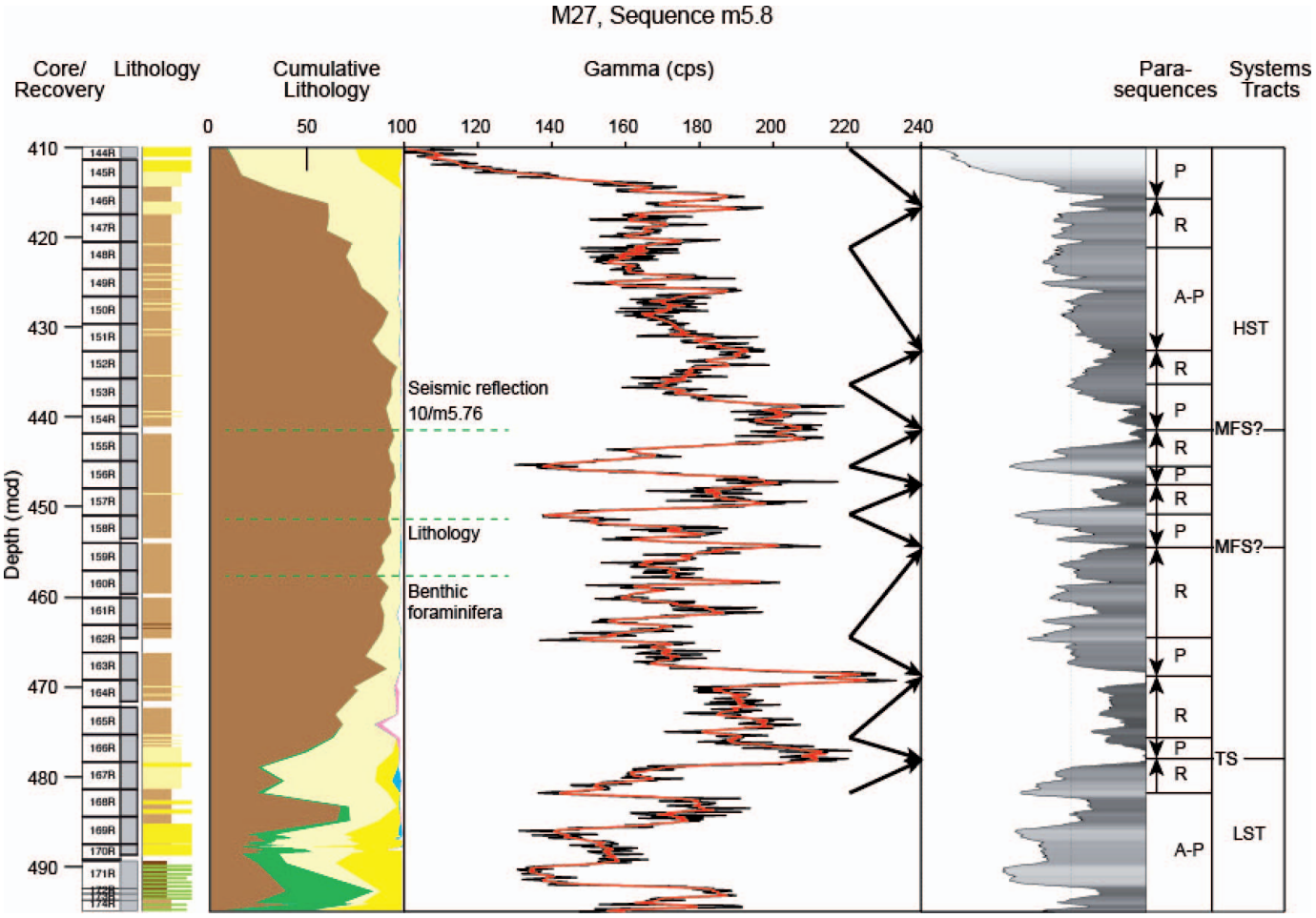

FIG. 8.—Gamma-log interpretation of sequence m5.8 showing parasequences. FS, flooding surface. Arrows point in fining direction. TS, transgressive surface; MFS, maximum flooding surface; R, retrogradational parasequence; P, progradational parasequence; A, aggradational parasequence.

with previously published seismic stratigraphic predictions (Greenlee et al. 1992; Monteverde et al. 2008) of thick LST and thin to absent TST (Fig. 6). Miller et al. (2013b) noted that the Myr-scale sequence m5.4 (spanning ~ 17.7–16.7 Ma) is a composite sequence (composed of sets of higher-order sequences; *sensu* Mitchum and Van Wagoner 1991; Neal and Abreu 2009) that can be parsed into three higher-order sequences, m5.4/m5.4-1, m5.34, and 5.33. Here, we review the interpretation of lower Miocene composite sequence m5.4 and provide new interpretations of lower Miocene sequence m5.8 (19.2–20.1 Ma) that suggest that it, too, may be a composite sequence.

Industry Efforts in the BCT

The US Geological Survey (USGS) and industry seismically imaged and drilled the Continental Offshore Stratigraphic Test [COST] B-2 and B-3 stratigraphic test wells (Scholle 1977, 1980) and 32 exploration wells in the BCT (Libby-French 1984; Prather 1991). Exploration efforts focused along four trends:

1. Fault closures and traps on the middle shelf associated with the Great Stone Dome (GSD), a large, Early Cretaceous mafic igneous intrusion or dike swarm (Figs. 3, 4), provided a tantalizing target; seven dry wells were drilled on and off structure, and it is thought that igneous emplacement thoroughly fractured the section, destroyed potential traps, and enabled hydrocarbons to escape (Prather 1991).
2. Structures on the outer continental shelf (OCS; Fig. 4) yielded natural gas in 5 of 21 wells in sandstones and limestones at Texaco 598-1, Exxon 599-1, Texaco 642-1, and -3 and Tenneco 642-2, with a small amount of thermally immature oil in Albian sandstone in the latter well (Prather 1991).
3. A fringing reef largely beneath the continental slope and extending along most of eastern North America (Jansa 1981) was also an attractive target. Three wells drilled by Shell in oolitic grainstones in a flooded bank setting, anticlinal, fault-bounded rollovers, and pinnacle reefs (Karlos 1986) were dry.
4. Shelf-margin deltaic complexes provided additional targets; all proved dry. Shell drilled one dry well (93-1) south of Wilmington Canyon to test for hydrocarbons in fault-bounded clastics overlying a foundered portion of the shelf-margin carbonate trend (Prather 1991).

We accessed well-log and seismic data from these efforts (Fig. 9) and prepared gamma-ray-log sequence stratigraphic interpretations and correlations for the GSD and OCS, focusing on the Logan Canyon Formation, a succession of Aptian to lower Cenomanian sandstones and shales first identified and correlated by Libby-French (1984). Libby-French (1984) identified the upper Logan Canyon and lower Logan Canyon sandstones separated by the Sable Shale and correlated them through 19 wells in the northern Baltimore Canyon Trough. Similarly, Seker (2012) constructed well-log cross sections for 11 wells along the outer continental shelf, and Hlavaty et al. (2012) did the same for 6 wells across the GSD. These

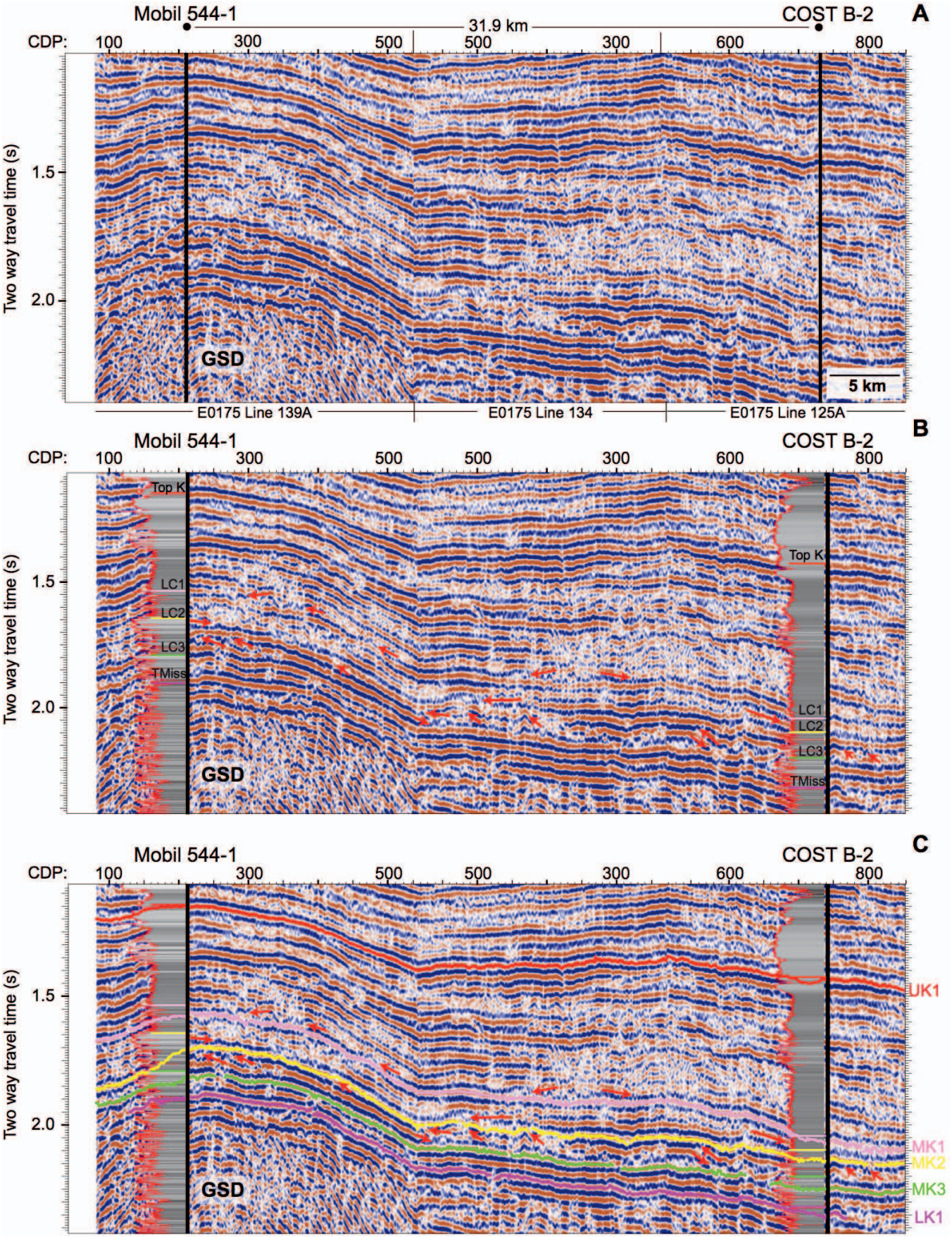
A
Mobil 544-1
31.9 km
COST B-2
CDP:
100
300
500
500
300
600
800
Two way travel time (s)
1.5
2.0
GSD
5 km
E0175 Line 139A
E0175 Line 134
E0175 Line 125A
B
Mobil 544-1
COST B-2
Top K
LC1
LC2
LC3
TMiss
GSD
C
Mobil 544-1
COST B-2
UK1
MK1
MK2
MK3
LK1
GSD

studies took a largely lithostratigraphic approach, though all tried to honor available biostratigraphy.

Here, we reinterpreted the well-log correlations by integrating gamma-ray-log data with biostratigraphy within a sequence stratigraphic framework that shows that the Logan Canyon consists of three sandstone bodies associated with three distinct sequences. Numerical values from gamma-ray logs were plotted with gray-scaled shadings such that the highest gamma-ray values are black and the lowest are light gray (Figs. 10–13), with shades of gray in between proportional to the gamma-log values. This approach yields optimal visualization of well-log stacking patterns, with the presumption that the gamma-ray logs in these siliciclastic sandstones and mudstones reflect mainly quartz sand versus mud content.

Our correlations of Logan Canyon sequences are based on interpretations of geophysical logs, seismic profiles, and biostratigraphy obtained from BOEM's (Bureau of Ocean Energy Management) data repository for the Atlantic margin. Age control uses planktonic foraminifera, calcareous nannofossils, and palynomorph biostratigraphy (pollens, spores, dinoflagellates) from original industry paleontology reports. The biostratigraphy was revised to acknowledge modern understanding of species ranges, specifically for the Aptian, and preference for Albian and early Cenomanian tops is given to species which are encountered in at least two wells. Though most biostratigraphic interpretations are consistent from well to well, some of the chronostratigraphic tops reported (particularly palynomorphs) were not compatible with our log correlations, and we opted instead to use select foraminiferal, nannofossil, and palynomorph highest occurrences (HOs) from 12 exploratory wells (Supplemental Fig. S2). The ages of HOs were determined using GTS2012 (Gradstein et al. 2012) for correlation with global bioevents. In the Logan Canyon Formation, four main bioevents were identified in each well and correlated across the margin (Supplemental Fig. S2). The scarcity of biostratigraphic index taxa in the older stratigraphic succession (below the Aptian) made it difficult to obtain an accurate age estimate, thus we restrict this study to the Aptian to Cenomanian Logan Canyon sequences. The biostratigraphic highest occurrences support the interpretation of three major Logan Canyon sequences that approximate the Aptian, Albian, and lower Cenomanian (Supplemental Fig. S2).

RESULTS

Miocene Sequence m5.4 Example

Previously studies have recognized sequence m5.4 based on seismic reflection terminations at its base and top (Fig. 5; Monteverde et al. 2008; Mountain et al. 2010; Miller et al. 2013a, 2013b). Browning et al. (2013) used integrated biostratigraphy and Sr-isotope stratigraphy to date sequence m5.4 as a ~ 1.2 Myr scale sequence (17.7–16.6 Ma), with short hiatuses at its base and top. Initial seismic studies interpreted a thick LST from the basal sequence boundary reflection m5.4 to a prominent downlap surface reflection m5.32 (Fig. 6; Supplemental Fig. S1; Monteverde et al. 2008). Before coring, m5.32 was initially interpreted as the MFS, with little to no TST and a thin HST above m5.32 to the overlying sequence boundary at reflection m5.3 (Fig. 6; Monteverde et al. 2008).

Coring and logging provided new constraints on interpretation of sequence m5.4 (Mountain et al. 2010; Miller et al. 2013a, 2013b). Chronostratigraphic control showed a 0.7 Myr hiatus associated with reflection m5.32 (17.4–16.7 Ma; Browning et al. 2013), prompting a reexamination of the seismic profiles and core stacking patterns. Interpretations of internal reflections in sequence m5.4 indicated that it contains three higher-order sequences, suggesting that m5.4 is a composite sequence consisting of three ~ 100-kyr-scale sequences, m5.4/m5.4-1, m5.34, and 5.33 (5.4-1 is a higher-order sequence that shares the same basal sequence boundary with the Myr sequence m5.4).

Here we provide both dip (Fig. 5A, B) and strike (Fig. 5C, D) views of sequence m5.4. We observe onlap onto reflections m5.34 and m5.33. A downward shift of onlap onto reflection m5.34 (479 mcd at Site M28) and erosional truncation of the underlying m5.4 sequence boundary including removal of sequence m5.4-1 at the updip Site M27 (Figs. 5, 6) indicate that m5.34 is a seismic sequence boundary, as also seen on adjacent profiles. Reflection m5.33 (405.0 mcd at Site M28) appears to be a sequence boundary, based on onlap and downlap (Fig. 5D). Though Miller et al. (2013b) did not report onlap on adjacent profiles, we illustrate a strike line through Site M28 that clearly shows terminations (erosional truncation, onlap) associated with m5.33 (Fig. 5C, D) that supports interpretation of this reflection as a sequence boundary.

The facies stacking patterns observed in cores (Fig. 6), benthic foraminiferal patterns, and age control strongly support the interpretation of higher-order sequences m5.4-1, m5.34, and 5.33.

1) Above the m5.4/m5.4-1 sequence boundary (512.3 meters composite depth (mcd)), there are two coarsening-upward, overall aggradational parasequences that are part of an 11-m-thick LST. A change from coarsening to fining and deepening upward (as indicated by foraminiferal proxies) occurs at the TS at 501 mcd. The fining-upward TST with two thin parasequences extends to 494.0 mcd at the MFS and then coarsens and shallows upsection in the HST to a major reflection ("7"/m5.34) at 479 mcd (Figs. 6). This regressive–transgressive–regressive stacking pattern supports the interpretation that m5.4-1 is a higher-order sequence (Fig. 6). There is no resolvable hiatus associated with the higher-order sequence boundary (17.6 Ma), and this may be our one example of a correlative conformity with no hiatus.
2) A LST over the m5.34 sequence boundary is indicated by a coarsening-upward succession immediately above reflection m5.34 at Site M28 to ~ 475 mcd at the TS (Fig. 6). Subsequent fining upward occurs from ~ 475 to ~ 468 mcd (Fig. 6) in the TST. Data on grain size and foraminifera cannot resolve the MFS, but close examination of the gamma-ray log reveals four progressively deeper parasequences (Fig. 8 in Miller et al. 2013b), with the MFS identified using gamma-ray logs at 449 mcd associated with a downlap surface (reflection "10," Fig. 6). The sequence coarsens and shallows upsection in the HST (449–405 mcd) with five progressively shallower parasequences indicated on gamma-ray logs by FS at 442, 435, 432, and 427 mcd (Fig. 6).
3) Above the m5.33 sequence boundary (405.0 mcd), a single coarsening-upward parasequence characterizes the LST (405.0–394.0 mcd) capped by a TS (Fig. 6). Above this, there is a thin fining-upward TST and a MFS (391.0 mcd) associated with reflection m5.32 and a gamma-ray peak. Coarsening (391.0–380.0 mcd) and seismic progradation marks the HST. Blocky, aggradational sands at the top of the sequence (380.0–361.0 mcd) are associated with downstepping reflections (Fig. 6; see Discussion section on FSST).

←

FIG. 9.—Industry dip-strike-dip profile connecting the Great Stone Dome (GSD; Mobil 544-1 on structure) and the COST B-2 well. Uninterpreted (Part A, top panel), interpreted with red arrows indicating onlaps, downlaps, erosional truncations, and toplaps (Part B, middle panel), and interpreted with three preliminary seismic sequence boundaries (MK1 (pink), MK2 (yellow), and MK3 (green; Part C, bottom panel) below the major Top Campanian (UK1) sequence boundary. Numbers on top are CDP. Logs at Mobil 544-1 and COST B-2 are interpreted gamma-ray logs, with the position of the top of sequences LC1, LC2, LC3, and top Missisauga.

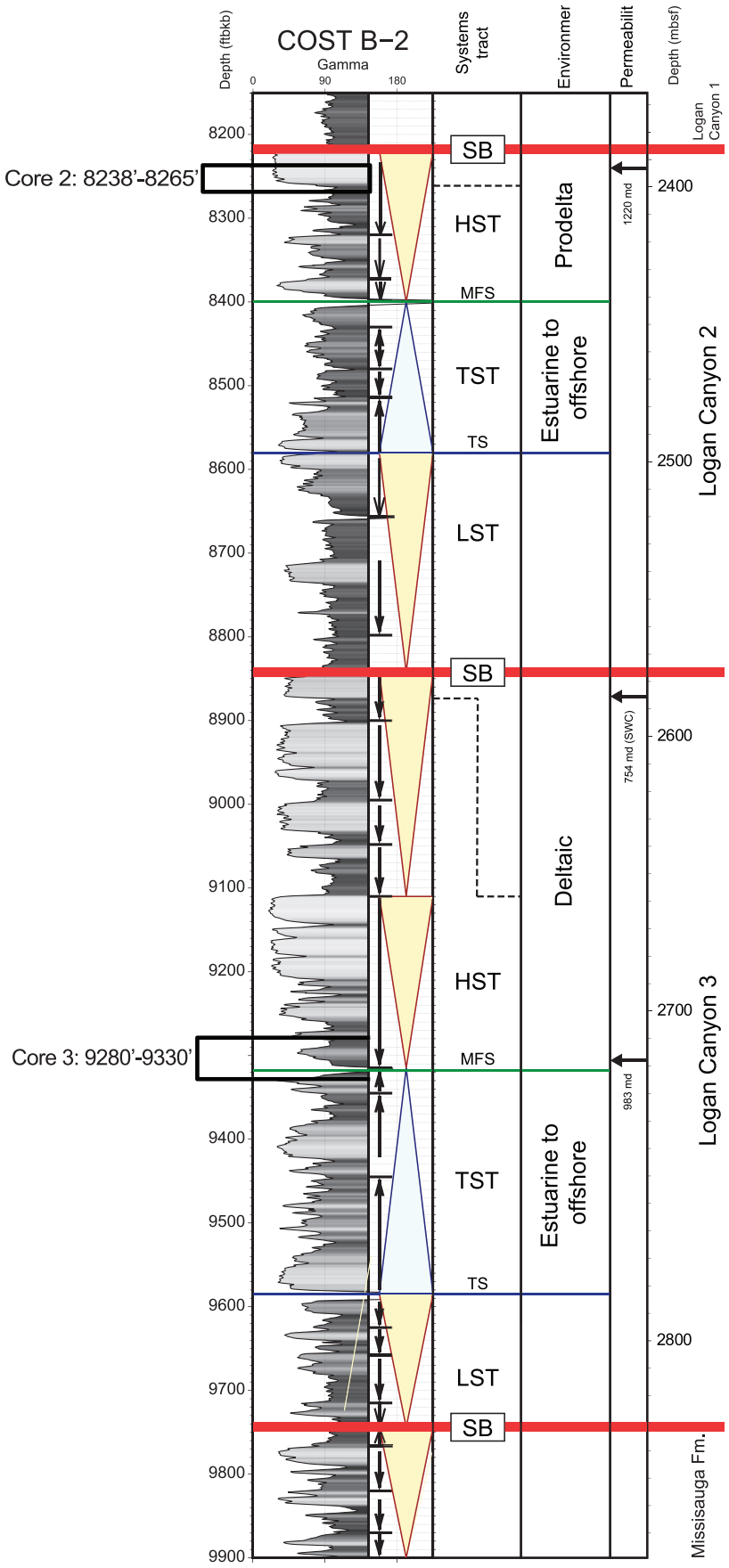

FIG. 10.—COST B-2 stratigraphic section. Grayscale-shaded well-log cross section of gamma-ray logs and sequence stratigraphic interpretation. High gamma-ray values are shaded black to dark gray and are indicative of muds or shales; medium gamma-ray values appear gray for muddy sands or sandstones or for finely interbedded units of mud/shale and sand/sandstone; low gamma-ray values appear light gray to white and are indicative of clean sands. Parasequences are represented by black arrows pointing in the fining direction and are bounded by flooding surfaces that are shown as horizontal lines. Large triangles are yellow for coarsening upward successions, and blue for fining-upward successions, and have been identified by parasequence trends (stacking patterns) and gamma-ray log spikes (often MFS, maximum flooding surfaces (MFS) or transgressive surfaces (TS)). Red lines are sequence boundaries (SB).

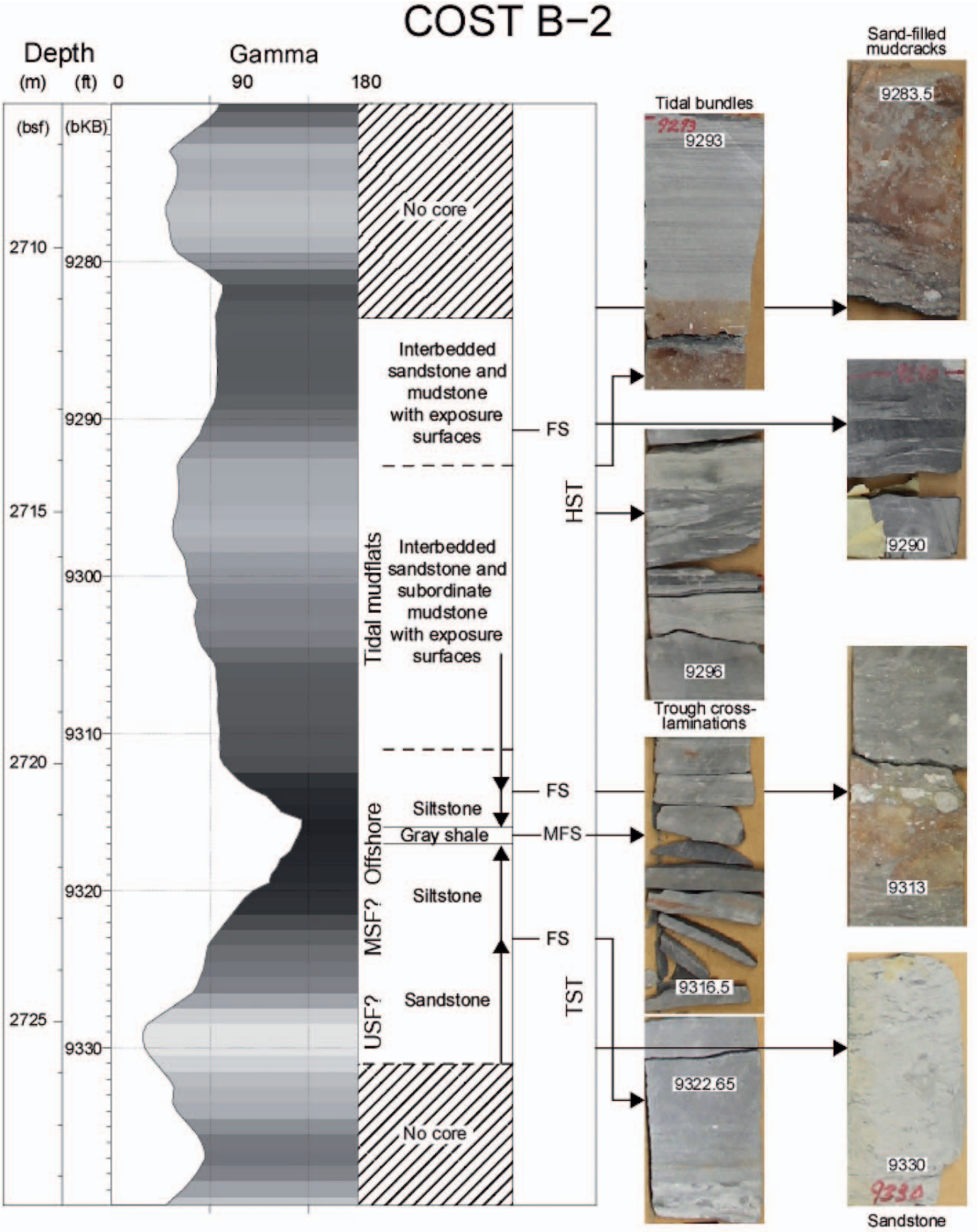

FIG. 11.—COST B-2 core ground truth. See Figure 9 caption for description of log display. FS, flooding surface; TS, transgressive surface; MFS, maximum flooding surface; TST, transgressive systems tract; HST, highstand systems tract.

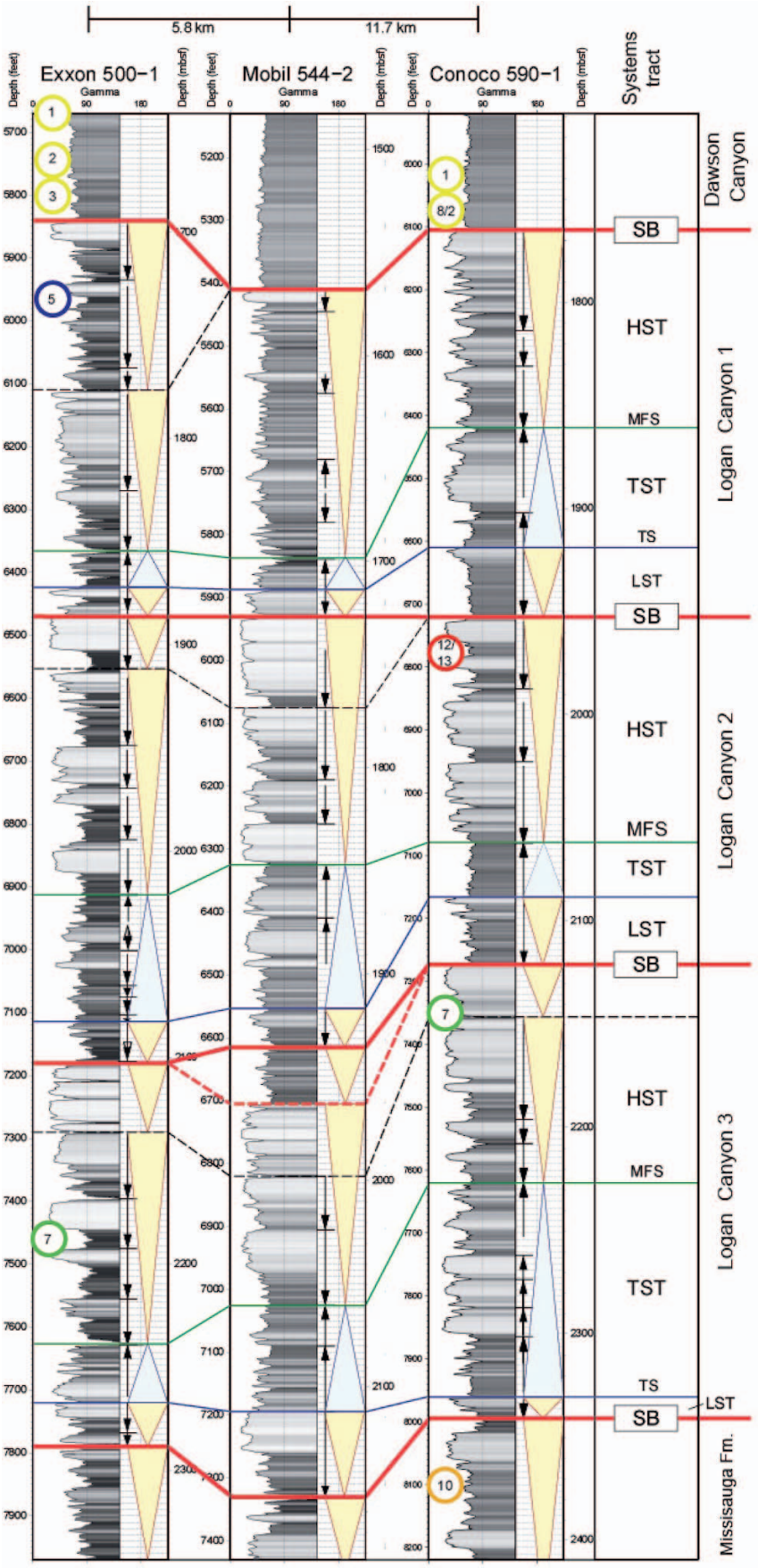

FIG. 12.—Example of well logs for the Logan Canyon Formation across the Great Stone Dome. Caption as in Figure 9. Depth (feet below Kelly bushing) is hung on the top of the Albian, as justified by biostratigraphy (Supplemental Tables S1 and S2; Supplemental Fig. S2). Biostratigraphic picks are shown in colors: yellow, upper to middle Cenomanian; purple, lower Cenomanian; red, top Albian; green, top Aptian; and orange-tan, Barremian. Numbers are keyed to biostratigraphic markers in Supplemental Tables S1 and S2.

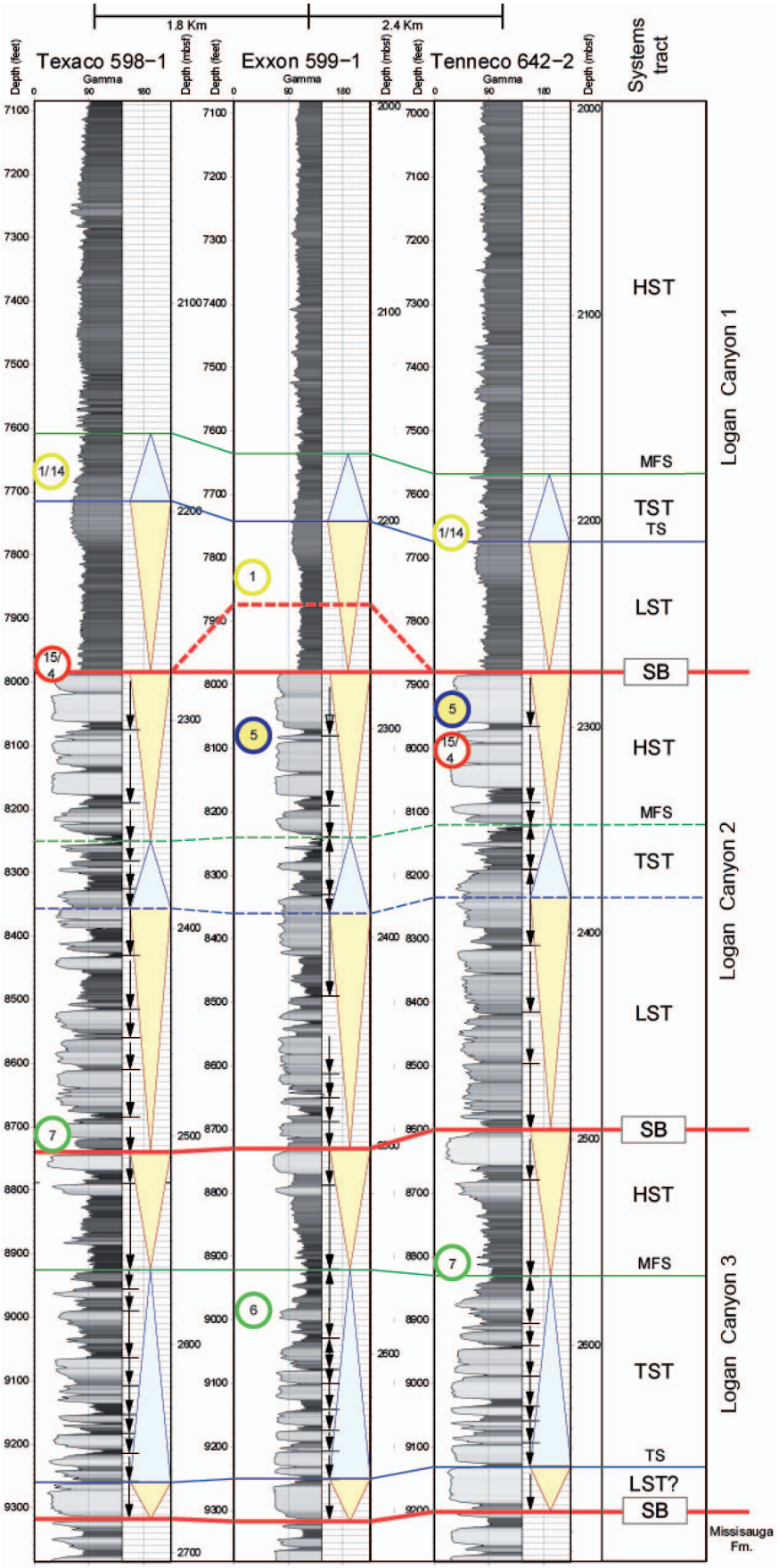

FIG. 13.—Example of well logs for the Logan Canyon Formation across the outer continental shelf. Caption as in Figure 9. Depth (feet below Kelly bushing) is hung on the top of the Albian as justified by biostratigraphy (Supplemental Tables S1 and S2; Supplemental Fig. S2). Biostratigraphic picks are shown in colors: yellow, upper to middle Cenomanian; purple, lower Cenomanian; red, top Albian; green, top Aptian; and orange-tan, Barremian. Numbers are keyed to biostratigraphic markers in Supplemental Tables S1 and S2.

Examination of *Oceanus* strike line 24 supports our interpretation of the higher-order sequence boundaries m5.4-1, m5.34, and m5.33 (Fig. 5C, D). Mapping of sequences on strike and dip lines shows thickening and thinning along strike (Monteverde 2008; Montverde et al. 2008). Reflection terminations of onlap, downlap, toplap, and erosional truncation are found along strike for the sequence boundaries (Fig. 5C, D). The strike line shows a particularly interesting feature above sequence boundary m5.33. From 2500–3700 Common Depth Point (CDP) (Fig. 5C, D) there is erosion associated with reflection m5.32, which is a MFS at Site M28 (Fig. 6). Steeply dipping reflections below m5.32 are likely artifacts (diffractions off the irregular surface), because they cut across a reflection between m5.33 and m5.32. The erosion on the MFS m5.32 surface is similar to the m5.8 MFS discussed below and may indicate that this surface is a higher-order sequence boundary merged with a MFS.

The age–distance (Wheeler 1958) diagram further emphasizes that the Myr m5.4 sequence is in fact three sequences (Fig. 6). All three sequences step seaward of the underlying sequence and then step landward. We emphasize that only by integration of seismic, core (grain size, benthic, % planktonic), and log data could the higher-order sequences be fully delineated.

Miocene Sequence m5.8

Previous studies used reflection terminations to show that reflection m5.8 is a seismic sequence boundary (Fig. 5A; Monteverde et al. 2008; Mountain et al. 2010; Miller et al. 2013a, 2013b). The top of sequence m5.8 is highly dissected by the overlying sequence m5.7, and there is a strong downlap surface on the bottomset (reflection 10/m5.76; ∼ 6500–6700 CDP, Fig. 7A) that is traceable along strike. Site M27 sampled sequence m5.8 in the foreset at its thickest point (133.6 m, Fig. 7A) and allowed dating it as 19.2–20.1 Ma, bracketed by short hiatuses (Browning et al. 2013).

Core–seismic integration is consistent with the interpretation of m5.8 as a single sequence. Two thin, upward-coarsening parasequences constitute the LST (494.87–477.52 mcd), with an increase in quartz sand from the lower to the upper parasequence. The TS at 477.52 mcd is associated with a prominent, high-amplitude reflection (number 3, Fig. 7A–C) that laps onto and laps down onto the seismic sequence boundary. The TS is overlain by a fining-upward TST with the MFS placed at 457.78 mcd as indicated by benthic foraminifera, at 451.36 mcd as indicated by the maximum in mud content based on core descriptions (Mountain et al. 2010), or at 442 mcd in association with reflection 10/m5.76 (Fig. 7A, B; Miller et al. 2013b). The section clearly coarsens upward above 430 mcd to fine sand at ∼ 415 mcd and above that to a blocky, aggradational medium–coarse sand that continues to the overlying m5.7 sequence boundary at 361.28 mcd (Fig. 7A; Miller et al. 2013a, 2013b; Ando et al. 2014).

We have traced sequence m5.8 using seismic data to onshore cores at Ocean View, New Jersey (Fig. 3; Miller et al. 2001), where it correlates with the Kw1a sequence. The latter has been divided into three higher-order sequences and is another example of a composite sequence, which prompted us to revisit the seismic interpretations of sequence m5.8 by looking more closely at internal reflections. The resolution of the *Oceanus* and *Cape Hatteras* seismic data is high enough to interpret major sequence boundaries (e.g., m5.8, m5.7, etc.) that exhibit clear reflection terminations (Fig. 5A, B). Seismic resolution is not high enough to unambiguously determine the internal nature of sequence m5.8 with the same level of certainty, hence allowing multiple seismic interpretations. Nevertheless, we have tentatively identified 18 internal reflections associated with sequence m5.8 (Figs. 7B, C). The internal reflections differ somewhat from those illustrated by Miller et al. (2013b), who identified only eight, though it is notable that our reflection 10/m5.76 is their reflection 5 that they interpreted as a MFS. The geometries of our internal reflections are intriguing, suggesting that there are higher-order sequences within sequence m5.8.

Based on the geometries present (Fig. 7C), sequence m5.8 appears be a composite of at least two seismically resolvable sequences. Reflection 3 is a strong seismic reflection identified previously as the TS and laps onto m5.8 seaward side of the clinoform rollover, and laps down on m5.8 farther seaward on the foreset. In fact, this reflection is likely a composite of the TS and lower TST as indicated by the change in impedance over a thick section (470–480 mcd; Miller et al. 2013a). Reflections 4 to 8 show progressive updip onlap of the TS and SB on its landward side (except for reflection 5, which is truncated by reflection 6), while the overlying reflection 9 is truncated by reflection 10/m5.76, the MFS of Miller et al. (2013b). This erosion suggests that reflection 10 is a sequence boundary merged with a MFS. In the seaward direction, reflections 4 to 6 lap down onto the TS and reflection 7 laps down on the SB, whereas reflection 10/m5.76 truncates reflections 8 and 9. The core data at Site M27 shows that reflections 3 to 5 are associated with upward fining in the TST and correlate to mud and muddy sand, whereas reflections 5–10 are in the MFS zone outlined by Miller et al. (2013b) and correlate to an interval of silt.

Reflection 10/m5.76 is interpreted as a MFS (Fig. 7C), though, as noted, there is seismic evidence that it might also be a higher-order sequence boundary (Fig. 7B). Reflections 11 to 18 both lap onto and lap down upon reflection 10/m5.76 and are associated with upward coarsening from silt to silty sand to sand. Onlap onto reflection 10/m5.76 is shown on the landward side (from ∼ 7300–7850 CDP) and on a portion of the seaward side (∼ 6400–6750 CDP). Evidence that reflection 10/m5.76 is a higher-order sequence includes the downward shift in onlap of reflection 11 on 10/m5.76, downcutting erosion (not just bypass or starvation as expected for a MFS) shown in the profile and in the Wheeler diagram, its general clinoform-shaped geometry (with a clinoform rollover at 6800 CDP), and the fan-shaped deposits on its toe (reflections 12–15; ∼ 6400–6750 CDP), interpreted as a higher-order lowstand deposit.

The section above reflection 10/m5.76 landward of the clinoform rollover at ∼ CDP 6750 is the HST (Fig. 7B). Downlap occurs on reflection 10/m5.76 landward of the clinoform rollover as expected in the HST and also on the seaward side of CDP 6750. On the landward side (∼ 7300–8000 CDP), the Wheeler diagram shows a progressive onlap from reflections 11 to 17 and three backstepping parasequences. Reflection 18 is truncated by sequence boundary m5.7. On the seaward side of the sequence, the discontinuous reflections transition from onlap to downlap onto reflection 10/m5.76, with onlap seaward of the clinoform rollover interpreted as a LST of the higher-order sequence (Fig. 7B).

Interpretations of gamma-ray-log stacking patterns further support interpretation of sequence m5.8 as a composite of at least two higher-order sequences (Fig. 8). Above the TS at 477.52 mcd, log parasequences are generally retrogradational to 455 mcd, between the levels assigned maximum water depth using benthic foraminifera (457.78 mcd; Katz et al. 2013) and that based on lithology (451.36 mcd). From 455 to 442 mcd (the level of reflection 10/m5.76; Fig. 8), the parasequences prograde, then sharply retrograde to the level of reflection 10/m5.76 (442 mcd), which is the best placement of the MFS. Parasequences generally stack progradationally above reflection 10/m5.76, as expected in the HST (Fig. 10). The two progradational stacked parasequences below reflection 10/m5.76 are consistent with a thin, truncated higher-order HST below, and the interpretation of reflection 10/m5.76 as both a higher-order sequence boundary and the lower-order Myr-scale MFS.

Though the internal seismic reflections and log stacking patterns suggest that reflection 10/m5.76 is a higher-order sequence boundary, sedimentological data provide no evidence for this interpretation. Reflection 10/m5.76 occurs at a 76 cm coring gap (441.15–441.91 mcd) with uniform silts above and below. There is no evidence for a hiatus associated with reflection 10/m5.76 (Browning et al. 2013). We thus also present an interpretation of sequence m5.8 as a single sequence and reflection 10/

m5.76 as a MFS (Fig. 7C), though we prefer interpreting sequence m5.8 as a composite of at least two sequences based on seismic and log evidence, with a third higher order sequence noted onshore truncated by overlying sequence boundary m5.7.

We emphasize that the ability to recognize higher-order sequences is strongly data dependent. Our interpretations of the internal reflections for sequence m5.8 as a composite sequence (Fig. 7B) on existing 2-D seismic data are reasonable, but not unequivocal. A 3D seismic grid that crosses the Expedition 313 drill sites is in the processing stage, and when complete it will allow us to test these interpretations and those for sequence m5.4.

Mid-Cretaceous Example
Seismic Interpretations

We evaluated seismic, core, and well-log data from the GSD to OCS targeting porous sandstone reservoirs of the Logan Canyon Formation, a series of Aptian to lower Cenomanian sandstones and shales (Libby-French 1984), for carbon storage. Our initial evaluation of USGS and Exxon MCS data failed to show clear reflection terminations between subparallel seismic reflections, largely due to limitations in seismic resolution (> 25 m vertical resolution). Newly released industry seismic data show reflection terminations within the Logan Canyon Formation that allow us to evaluate the seismic sequence stratigraphy of this unit from the GSD to the COST B-2 well in the northern BCT (Fig. 9). Using reflection terminations, we identified and traced three preliminary seismic sequence boundaries (MK1 (pink), MK2 (yellow), and MK3 (green); Fig. 9) below the major top Campanian (UK1) reflection and above a Barremian unconformity first reported by Lippert (1983). MK1, MK2, and MK3 all show downlap, with common onlap on MK2 and possibly MK1, and erosional truncations associated with MK2 (Fig. 9). Our seismic criteria show that MK2 is a clear seismic sequence boundary and MK1 and MK2 are likely sequence boundaries, consistent with the gamma-log-based interpretations described below. Profiles have been tied to wells using checkshots, vertical seismic profiles, and synthetic seismograms and show good correlation (within 100 ft; 33 m) to sequence boundaries LC1, LC2, and LC3 identified in gamma logs and described below.

COST B-2 Rosetta Stone

The COST B-2 well is among the most intensely studied offshore well, and though few cores were collected at this site, there is an especially complete set of logs (Figs. 10, 11). Examination of COST B-2 cores at the Delaware Geological Survey (DGS) and integration of core description and core photographs with gamma-ray logs (Figs. 10, 11) provides constraints on the environments of deposition and sequences in the Logan Canyon Formation. Core 3 (9285–9330 ft below Kelly bushing [ftbKB]; 2712.5–2726.4 meters below sea floor [mbsf]. We use ftbKB as logging units to ensure compatibility with previous studies [e.g., Scholle 1980; Libby-French 1984] but provide depths converted to meters below seafloor for ease of comparison with seismic profiles.) from the COST B-2 well sampled a portion of a depositional sequence that includes the upper part of a TST, MFS, and the lower part of a HST of the Logan Canyon 3 (LC3) sequence (Fig. 11). Sedimentological features indicating a marine setting include the following succession from the base upwards:

1) Homogeneous to laminated sandstone (Fig. 11) with *Ophiomorpha* burrows, indicating deposition in shoreface (likely upper shoreface) environments, are overlain by siltstone beds that we interpret as deposited in deeper shoreface to offshore environments and are thus transgressive; two parasequences are observed in the core in the TST separated by a FS at 9323 ft (Fig. 10; 2394 mbsf) with cross-bedded sandstones overlain by laminated siltstones (Fig. 11);
2) Laminated very dark gray shales are associated with a gamma-ray-log peak; we interpret the darkest of these shales at 9316.5 ft (2722.1 mbsf; Fig. 11) as the MFS deposited in offshore environments;
3) Trough cross laminations (Fig. 10), sand-filled mud cracks (Fig. 10), bundles of laminations, lenticular beds, soft-sediment-deformation features, and exposure surfaces (Fig. 11) all suggest an interpretation of deposition in tidal mudflats of the lower HST; the bundling varies from thinly laminated to thickly laminated and is tentatively interpreted as astronomical spring and neap tidal bundles (Fig. 11). Two parasequences are indicated by a shallowing-upward trend with exposure surfaces overlain by deeper-water laminated siltstones interpreted as an offshore environment associated with the FS (Fig. 11).

Placing the core-log observations into a full sequence stratigraphic context (Fig. 10) allows us to interpret three sequence boundaries in the Logan Canyon Formation at COST B-2. Stacking patterns are a way to extend the interpretation of lithofacies beyond the cored interval using well logs, particularly gamma-ray. Black arrows are shown next to the log data to indicate the inferred fining direction in each parasequence.

The LC3 sequence is the lowermost of the three Logan Canyon sequences (Fig. 10; sequences are numbered with 1 at the top). The basal LC3 sequence boundary is placed at 9745 ft (Fig. 10) at a sharp change from a regressive HST below to a FS at the base of a series of four parasequences that progressively coarsen up to a TS at 9585 ft (2804.0 mbsf). The environmental setting is uncertain for the calcareous shales and sandstones reported from this section from cuttings (Scholle 1980), though a tidal environment similar to that of the calcareous shales above the MFS (Fig. 11) is reasonable, and we speculate that this section represents an incised-valley fill. The overlying TST consists of three fining-upward parasequences, culminating in the MFS at 9316 ft (2722.0 mbsf; Fig. 10) as seen in core 3 (Fig. 11). The uppermost unit of LC3 is the HST comprising five coarsening-upward parasequences with blocky, aggradational sandstones at the top. Several lines of evidence indicate the HST consists of deltaic deposits, most likely delta front environments. We base this on the trend of upsection shoaling (Figs. 10, 11) supported by descriptions of alternating porous clean sandstones, lignitic sediments with calcareous shales, and shaly limestones deposited in recurring tidal-flat environments (Scholle 1977). The log patterns at COST B-2 display classic river or wave-dominated deltaic stacking (Van Wagoner et al. 1990) where sand intervals thicken upward, percent sand increases upward, and there are sharp upper contacts with abrupt shifts to finer-grained facies at flooding surfaces (parasequence boundaries).

The LC3 as defined here is partly equivalent to the lower Logan Canyon sandstone of Libby-French (1984). However, the genetically related shales in the lower LST below 9680 ft (2833.0 mbsf) were placed by the latter in the underlying Naskapi Shale, illustrating the differences between a sequence stratigraphic and lithostratigraphic approach. This sequence is Aptian based on the highest occurrence of the dinoflagellate cyst *Cyclonephelium tabulata* in core 3 (Fig. 11; 9290 ft; 2714.0 mbsf), with an age of ~ 118 Ma (Supp. Fig. 1). This is the thickest of the LC sequences at COST B-2 and is the most sand prone, with porous (~ 30%) permeable (Scholle 1980; Supplemental Fig. S3; 754 mD at 8870 ft [2704.3 mbsf] and 983 mD at 9305 ft [2836.9 mbsf]) sandstones.

The Logan Canyon 2 (LC2) basal sequence boundary is placed at 8845 ft (2696.6 mbsf) at COST B-2. The base of the sequence consists of shales that coarsen upwards to sandstones in two parasequences. The TS is placed at a thin shale at 8582 ft (2616.5 mbsf) that represents a change in stacking from coarsening up (progradational) to fining up (retrogradational). Parasequences above the TS are poorly defined by lithofacies but aggrade upward and are bounded by a distinct gamma-ray-log maximum at the MFS at 8400 ft (2578.4 mbsf). The HST consists of three coarsening-upward parasequences, culminating in a blocky, porous, very permeable

(26.5% and 1220 mD at 8240 ft, 2512.2 mbsf; Supplemental Fig. S3) sandstone. The shales in the LST were assigned to the Sable Shale by Libby-French (1984) and the sandstones above to the upper Logan Canyon by Libby-French (1984). The sequence is entirely within the Albian, as indicated by the HO of *Favusella washitensis*, *Planomalina buxtorfi*, and *P. cretacea* at 8200 ft (2500.0 mbsf; Scholle 1980; Supplemental Fig. S2). The blocky sandstones have been identified previously as a potential target for carbon storage (see Discussion; D. Schrag, written communication 2012).

The Logan Canyon 1 (LC1) sequence at COST B-2 lacks the thick sandstones that are present updip on the GSD (Fig. 12) but is similar to the downdip OCS wells that also lack sandstones (Fig. 13). Nevertheless, stacking patterns allow us to infer a coarsening-upward LST, a fining-upward TST, a MFS, and two coarsening-upward parasequences in the HST (Fig. 11; Supplemental Fig. S2). The LC1 sequence was assigned to the Dawson Canyon Shale by Libby-French (1984), again emphasizing the difference between lithostratigraphic correlations and sequence stratigraphic correlations. The LC1 sequence is lowermost Cenomanian based on the Highest Occurrence (HO) of *F. washitensis* at 8200 ft (2500.0 mbsf; Scholle 1980; Supplemental Fig. S2).

We place the sequence boundaries at the tops of blocky sands in LC3 and LC2 at COST B-2 (Fig. 10) and other wells (Figs. 12, 13, Supplemental Fig. S2). While it is possible to place the sequence boundary at the bases of these blocky sands, we favor placing them at the tops:

1) These blocky sands are the stratigraphically highest parasequences of generally coarsening-upward parasequence sets in sequences LC3 and LC2 and thus appear to be genetically related.
2) The sand–shale contact at the top of the blocky sands is regionally traceable on wells (Figs., 12, 13; Supplemental Fig. S2).
3) On seismic profiles, the blocky sands at the top of LC3 correlate with the top of seismic sequence boundary MK3 (Fig. 9), though the correlation of the top of the blocky sands with the top of seismic sequence MK2 is ambiguous (e.g., correlating near the top sands at Mobil 544-1 but below at COST B-2; Fig. 9); and most importantly,
4) biostratigraphic data that indicate the blocky sands are the same biostratigraphic age as the underlying sequence (Figs. 12, 13; e.g., the SB at the top of LC 2 is associated with an Albian assignment at COST B2 and 5 other wells and the SB at the top of LC3 is associated with an Aptian assignment at two wells; Supplemental Fig. S2).

We plan further biostratigraphic and paleoecological studies to test theses correlations and assignments of shifting paleoenvironments from the blocky sands to the heterolithic shales–sandstones and shales above.

Well-Log Transect Across the GSD

We applied the procedures outlined for the COST B-2 well to the 7 wells spanning the GSD and 4 on the OCS (Supplemental Fig. S2). For clarity (Fig. 12), we focus on the well-log interpretation of two wells on the GSD (Exxon 500 and Mobil 544-2 just off structure) and one on its flanks (Conoco 590-1) in a down-basin-dip transect. Sequences are discussed from the lowest (LC3) upsection.

As at the COST B-2 well, the LC3 sequence is the most sand-prone sequence that we describe on the dip transect (Fig. 12) and throughout the GSD (Supplemental Fig. S2). The LST of the LC3 is identified by one to three coarsening-upward parasequences (Fig. 11, Supplemental Fig. S2) and the LST thins downdip across the GSD (Fig. 11, Supplemental Fig. S2). The TSTs consist of one to five fining-upward parasequences that thin and decrease in number onto the GSD structure (Fig. 11, Supplemental Fig. S2); the thinning is probably due to onlap, though this is not resolvable on the available seismic data (Fig. 9). The HST consists of several coarsening-upward parasequences and is relatively continuous in thickness (Fig. 12, Supplemental Fig. S2). Blocky, aggradational sandstones cap the sequence (Fig. 12). We are uncertain where exactly to place the top of sequence LC3 at Mobil 544-2 (Fig. 12) as well as at four other wells on the GSD (Supplemental Fig. S2). There is a coarsening-upward shale unit on top of the blocky sandstone at all the GSD wells that could be tied to either the LC3 HST or to part of the LST of an overlying sequence. As at COST B-2, the log data of the HST all show classic river and wave-dominated deltaic stacking patterns with the sand intervals thickening and increasing in percent sand upward, with sharp upper contacts and abrupt shifts to finer-grained facies.

These sandstones have the potential to be excellent reservoirs for carbon storage. High porosities and permeabilities were measured on the LC3 and LC2 HST sandstones at COST B-2 (Scholle 1977; Supplemental Fig. S3). Our well correlation suggests that the original porosity and permeability of sandstones on the GSD may yield similar excellent reservoirs and that the overlying sequence boundary and attendant mudstones provide a reliably intact confining unit. Though we cannot state that individual sandstone beds are traceable or whether lateral variations in diagenesis might affect original porosity and permeability of sandstones, the sequence stratigraphic framework allows us to predict thick, sandstone-prone zones just below the overlying sequence boundary.

The overlying Logan Canyon 2 (LC2) sequence has features similar to LC3. LC2 is also sand prone, beginning with a shale-rich LST that thins onto the GSD but thickens downdip at Conoco 590-1 and farther into the basin. In contrast to the LC3, the LC2 TST thickens onto the GSD. The HST again remains relatively constant in thickness and displays similar river or wave-dominated deltaic gamma-ray-log stacking patterns, not only on the GSD (Fig. 12) but also across the shelf to the COST B-2 well (Fig. 10) and the OCS (Fig. 13). Peak permeabilities ($>$ 1000 mD) were measured in the porous, blocky sandstones at the top of the sequence at COST B-2 (Scholle 1980), and again similarly high values might be expected at the wells at the GSD. There is some variability in the continuity and thickness of these sandstones (e.g., there are five to seven sand zones on the GSD wells; Supplemental Fig. S2), and storage capabilities may thus vary from well to well, but like the LC3, the LC2 sequence is an excellent candidate for carbon storage. These HST sandstones were generally included with the upper Logan Canyon on the GSD by Libby-French (1984). However, as shown on Supplemental Figure S2, the Sable Shale defined by Libby-French (1984), separating the upper and lower Logan Canyon, was placed both above and below the basal LC1 sequence boundary as we traced it, highlighting ambiguities in tracing the shale and lithologic units in general. By keying on the stacking patterns and sequence boundaries within a biostratigraphic framework, we avoided problems in tracing individual sandstone and shale units.

The Logan Canyon 1 (LC1) is sand prone on GSD, and becomes more shale prone seaward. On the GSD, the LC1 has a thin LST that thickens downdip, whereas the TST thickens downdip to Conoco 590-1 and cannot be readily identified on logs in the shale downdip from that. The HST is again relatively constant in thickness, but is not as sand rich as the underlying sequences. Sandstone zones are also less correlatable in the LC1 than the sequences below. The LC1 sequence is capped by thick Dawson Canyon shales that provide an apparently impermeable seal for the underlying sandstones (Libby-French 1984). It is interesting to note that the Cenomanian sandstones of the LC1 sequence pinch out by the COST B-2 well and are generally retrogradational compared to the underlying LC2 and LC3 sandstones. The "shaling out" of the sequence meant that previous studies have correlated the LC1 sandstone updip with the LC2 sandstones downdip. This miscorrelation could be avoided only by the use of sequence stratigraphy integrated with biostratigraphy.

Well-Log Transect Across the OCS

We have analyzed seven wells in a transect across the Outer Continental Shelf (OCS); three are along a dip profile and are interpreted in Figure 13,

and the other four are shown in Supplemental Figure S2. In all cases, depositional sequences LC3 and 2 are sandstone prone and LC1 is shale prone, as they are at COST B-2 (Fig. 13). The sequence boundaries for the base of LC1 and LC2 are at the top of blocky, aggradational sandstone overlain by coarsening-upward, predominantly shale packages; biostratigraphic picks reinforce the placement of the LC1 and LC2 sequence boundaries (Supplemental Fig. S2). The base of the lowermost LC3 sequence is less clear. On the GSD, it is placed at the base of a coarsening-upward parasequence (a gamma-log low), overlying more heterolithic strata of the underlying Missisauga Formation. Downdip on the edge of the GSD through OCS, the basal LC3 sequence boundary is placed at a thin shale beneath a thicker coarsening-upward sandstone (a gamma-log high), as supported by Barremian biostratigraphic picks immediately below this level (Supplemental Fig. S2). The differences in the log character (low vs. high) of the interpreted base of LC3 updip and downdip make this interpretation less certain than that of the base of LC2 and LC1.

The LC3 depositional sequence has a thin LST on the OCS that is thicker at COST B-2 and many of the GSD wells, though it is sandier downdip. The TST is thick and sandy and fines up to the MFS across the OCS. The HST is distinctly more shaly on the OCS than at COST B-2 except for a blocky sandstone at its top.

The LC2 depositional sequence has a very thick LST on the OCS that thins toward COST B-2 and further onto the GSD (Fig. 13). It comprises four or five blocky parasequences that do not readily correlate from well to well (Fig. 13). The TST is thin at all wells (Fig. 13). The HST is moderately thick and relatively uniform in thickness and consists of blocky sandstones particularly at the top of the sequence (Fig. 13). The HST appears to be an excellent reservoir on the OCS (as it is farther landward over the GSD) and is a potential target for carbon storage.

As previously noted, the LC1 depositional sequence is composed predominantly of shale on the OCS. A thick LST is indicated by an upsection coarsening at all of the OCS wells (Fig. 13). The TST appears to be thin at all wells, though the MFS is poorly defined, as is the upper depositional sequence boundary.

DISCUSSION

Back to Basics: Importance of Age Control and Integration of Methods

The Miocene and mid-Cretaceous examples presented here show application of reflection termination and stacking patterns to objectively recognize Myr-scale (and potentially shorter-period) sequences. It is important to recognize the scale of our focus, because we do not detract from using transgressive–regressive cycles (e.g., Embry and Johannessen 1992) or "genetic stratigraphy" (cycles bounded by MFSs; Galloway 1989) on longer time scales and larger spatial scales. Previous studies have shown that these approaches are useful for regional basin-scale stratigraphy, but they lack the resolution for reservoir-scale interpretation as provided here.

All of the interpretations discussed here were based on interpretations of data using basic stratal patterns that are not tied to assumptions about the position of relative sea level. Though we key on stratal patterns to interpret transgression and backstepping and regression and progradation, these are not necessarily related to relative sea level because they may reflect changes not only in accommodation, but also in sediment supply (Vail et al. 1977). We show that sequence boundaries can be objectively picked on seismic profiles by reflection terminations, downward shifts in onlap, and geometry of units on age–distance (Wheeler) diagrams (Figs. 5–7). On well logs, stacking patterns identify fining- and coarsening-upward successions that can be used to interpret systems tracts and stratal surfaces (Figs. 10–13). This approach avoids lithostratigraphic correlations that are often time transgressive, though a biostratigraphic framework is needed to support sequence stratigraphic studies. Similarly, with continuous cores, stacking patterns and chronostratigraphic control can be used to identify surfaces that are ambiguous using seismic or well-log data alone, such as cases in which the sequence boundary separates HST regressive sandstones from LST regressive sandstones of an overlying sequence (e.g., Figs. 6, 7A). We emphasize the importance of the integration of all available methods, seismic profiles, core lithology (grain-size trends, bioturbation), paleodepth indicators (sediment facies, benthic biofacies, % planktonics of total foraminifera), well logs (especially stacking patterns, e.g., Fig. 8), and chronostratigraphic control (biostratigraphy, Sr-isotope stratigraphy, other methods). Not all methods are available to address all sequence stratigraphic problems (e.g., detailed grain size, paleontology, and sedimentary facies changes such as Fig. 6 and 7A are possible only on core material which is very rare in industry applications). Ultimately, the recognition of sequences on any scale is data dependent, with the ability to resolve a sequence at a given scale heavily reliant upon the resolution of the data.

Implications for Reservoir Evaluation and Carbon Storage

Our interpretations of seismic profiles and well logs for the northern Baltimore Canyon Trough reinforce previous geological interpretations of excellent reservoir and seal potential for the mid-Cretaceous in this basin. Source rocks for petroleum are poorly developed in the basin and though there is natural gas in the OCS wells, it was not deemed economical (Prather 1991). The situation could not be more fortuitous for carbon storage. Carbon is best stored in subsurface reservoirs as a supercritical fluid, with initial structural trapping transitioning to mineralization over centennial to millennial time scales (Metz et al. 2005). Supercritical CO_2 requires a burial pressure greater than 7.38 MPa at temperatures $> 31.1°C$ (Bachu 2000); assuming a typical geothermal gradient of 25°C/km, 12°C surface temperatures, and a lithostatic gradient of 27 MPa/km, supercritical storage requires burial depths $>$ 800 m (Bachu 2000). Since the supercritical CO_2 drives off ambient pore fluids, it is not ideal to inject into natural-gas reservoirs unless gas recovery is targeted. Storage requires good seals that avoid leakage along faults or into existing exploration wells. In addition, earthquake stimulation is a concern for injecting supercritical fluids (Zoback and Gorelick 2012), and there are citizen concerns about onshore storage (Van Noorden 2010).

Our studies show that the Logan Canyon sandstones are a world-class candidate for storage. Based on core and sidewall core analyses (Scholle 1980), they are porous ($\sim$ 30%), very permeable ($\sim$ 1000 mD), and interconnected sandstone reservoirs capped by shale seals (Supplemental Fig. S3). The potential reservoir interval extends at least from the GSD to the OCS, a distance of $\sim$ 60 km (Fig. 4). The Logan Canyon sequences show little evidence for faulting and have few wells through it. Pumping supercritical CO_2 into the depths of the Logan Canyon, which is a poorly indurated unit, is not likely to exceed lithostatic pressures and cause fracturing and earthquakes. In addition, the offshore location offers several advantages compared to onshore storage by avoiding the public perception of concerns about storage beneath a populated area and reducing the difficulty of establishing surface and mineral rights at candidate storage sites (Litynski et al. 2011). The Logan Canyon sequences examined here appear to be suitable for storage from the GSD to the OCS, though the OCS sites are perhaps less desirable due to the presence of gas in the underlying Missisauga sandstones (Prather 1991; Seker 2012).

The Correlative Conformity?

In their study of the New Jersey lower to middle Miocene, Miller et al. (2013b) found little evidence for correlative conformities on the shallow ($<$ 100 m paleodepth) New Jersey continental shelf sampled by Expedition 313. Browning et al. (2013) showed evidence for hiatuses on the foresets (where sequences are most complete and correlative conformities are most likely) for m5.8, m5.4, m5.33, and m5.2 sequence boundaries of 0.3, 0.2,

0.7, and 0.7 Myr, respectively. Hiatuses on the topsets are longer than expected due to the absence of LST and hiatuses on bottomsets that were eroded or bypassed as a result of downslope transport processes. In this report, we have summarized evidence of erosion and hiatuses on Wheeler diagrams even in sections where sequences are physically most complete (Figs. 6, 7). However, there is no discernible hiatus associated with sequence boundary m5.34 (Fig. 6), the Wheeler diagram suggests possible continuity (Fig. 6), and this may in fact be an example where deposition was continuous, at least on the 100 kyr scale. Deep-sea sections adjacent to continental margins (e.g., continental slopes and rises) have intervals with short hiatuses or even apparently continuous deposition (Mountain et al. 1996; Pratson et al. 1994), but even there, hiatuses and downslope transport are often associated with sequence boundaries (Miller et al. 1996). Mountain et al. (2007) and Miller et al. (2013b) discussed slope deposition, conformities, and unconformities in more detail. We agree with Ager (1973) that, in shallow-water successions, there is often "more gap than record." Though we conclude that correlative conformity in time is largely unfounded and should not be considered a cornerstone of sequence stratigraphy, we concede that unconformities can be traced into "correlative surfaces" with no obvious erosion. Thus, we would agree with the emendation of the definition of depositional sequence to include "unconformities or their correlative surfaces" (Abreu et al. 2014).

The Falling-Stage Systems Tract

The falling-stage systems tract (FSST; Plint and Nummendal 2000) is widely used but controversial, especially with its relationship to the locations of the associated sequence boundary (see summary in Coe 2003), changes in relative sea-level, and to the underlying HST and overlying LST (Fig. 1). Vail et al. (1977) first termed all strata seaward of the clinothem rollover (Fig. 2; his "shelf break") as lowstand deposits. Although many studies have defined the LST in terms of sea-level curves (Vail 1987; Van Wagoner et al. 1987, 1988; Posamentier and Vail 1988; Posamentier et al. 1988; Coe 2003), there is general agreement that sediments of the LST lie directly on the sequence boundary, are the lower regressive systems tract containing aggradational to progradational parasequence sets, generally shallow up to the TS, and are largely restricted to the foreset and bottomsets (Fig. 2; Vail 1987; Van Wagoner et al. 1987; Posamentier et al. 1988; Coe 2003; Neal and Abreu 2009). In the FSST, strata both prograde as in the underlying HST and step down into the basin (often with sharp-based sands) as in the LST, and offlap progressively seaward (Plint and Nummendal 2000), with progradation and progressively steepening foresets (e.g., Proust et al. 2001). This is partly equivalent to the forced regression of Posamentier et al. (1992) and contrasts with the HST where strata progressively onlap landward (Plint and Nummendal 2000). There may not be a distinct surface separating the degradational FSST from the underlying HST (Plint and Nummendal 2000), but there may be a regressive surface of marine erosion (Proust et al. 2001; Trincardi and Corregiari 2000; Rabineau et al. 2005). In general, the sequence boundary is placed at the top of the FSST (Plint and Nummendal 2000), although placement of the base is "controversial" (see Coe 2003, p. 86).

In our Miocene examples, seismic criteria allow differentiation of sequence boundaries from surfaces and facies possibly associated with FSST. Possible FSSTs are recognized below seismic sequence boundaries just landward of clinoform rollovers associated with sequence m5.45 below sequence m5.4 (Fig. 6; with apparent downstepping of reflections 1 to 3), with the top of sequence m5.4 (Fig. 6; with apparent downstepping of reflections 17 to 20), and possibly in m6 below m5.8 (Fig. 7, with apparent downstepping of the reflector below m5.8). Where sampled at Site M28 in sequence m5.4, these possible FSST are blocky sands. However, in all three cases, the overlying sequence boundary can be objectively recognized by onlap, downlap, erosional truncation, and toplap and can be clearly differentiated from the underlying candidate FSST. Because the apparent downstepping geometry observed in the three examples above can also be explained by erosion by overlying reflectors (Fig. 6), we have avoided application of the term FSST, though we concede that the systems tract may have validity.

What is the Role of Sea level in Sequence Stratigraphy?

We have long been advocates that changes in relative sea level can be interpreted from passive-continental-margin records and that the similarities of sequences globally speak to a role for changes in global mean sea level (e.g., Miller et al. 2005). The cycle charts of Exxon (Haq et al. 1987; Haq 2014) remain useful for providing the ages of sea-level events, but they are misleading and meaningless in terms of amplitudes, as we have shown previously (Christie-Blick et al. 1990; Miller et al. 2005). Even the concept of eustasy as sea-level change defined "relative to the center of the Earth" (Posamentier et al. 1988) or to "some fixed datum" (SEPM, http://www.sepmstrata.org/TerminologyList.aspx?pg=2&search=) is fundamentally flawed and in fact misleading (Mitrovica 2009). Still, various processes, most notably ice-sheet growth and decay, do produce large, rapid, and nearly synchronous global changes in mean sea level that leave an indelible and common imprint on the stratigraphic record. The amplitudes and expressions of these changes in mean sea level varies regionally and locally, but commonalities are still expressed even in tectonically active settings (Bartek et al. 1991). We conclude that changes in relative sea level provide a strong influence on the development of depositional sequences but should not drive interpretation of sequence stratigraphy.

We have previously linked Miocene sequences to relative sea-level change (Miller et al. 2005, 2017). We also are intrigued about our mid-Cretaceous example, where we have identified three sequences in the ca. 20 Myr of the Aptian to earliest Cenomanian. Age control on these sequences is limited to sparse foraminiferal, dinocyst, and pollen data, and we are engaged in evaluating the biostratigraphy of the industry wells further. At this point we can state that the LC1 is Aptian (ca. 120–114 Ma), the LC2 is Albian (ca. 110–105 Ma), and the LC1 is earliest Cenomanian (ca. 100–98 Ma). This would suggest that their basal sequence boundaries correlate with the global record of major sequence boundaries reported by Haq (2014) at ca. 125.6, 113.3 to 109.3, and 100.5 Ma (Haq 2014). This preliminary interpretation requires further testing.

What Is a Depositional Sequence?

The ISSC Working Group on Sequence Stratigraphy discussed sequence stratigraphy for seven years and disbanded without reaching a consensus on the definition of a sequence (Salvador, written communication, November 11, 1998). Recent community attempts at standardization of the term "stratigraphic sequence" as "a succession of strata deposited during a full cycle of change in accommodation or sediment supply" (Catuneanu et al. 2009) also fail to provide objective criteria on which to define a sequence and again rely on accommodation, which is similar to, if not identical to, the concept of changes in relative sea level (Posamentier et al. 1988). The definition of a "depositional sequence" by Mitchum (1977) of "a relatively conformable succession of genetically related strata bounded by unconformities or their correlative. . ." [surfaces] still provides the most objective criteria, though as noted, we find little evidence for a correlative conformity in our data. We also note that the term "unconformity" means a surface of erosion or nondeposition of implied regional extent, in order to differentiate it from other more localized erosional surfaces (e.g., a TS, a channel, or a slump surface). In this contribution, we have striven to show that fundamental and objective seismic, lithologic, paleontological, and log criteria can be used to identify sequence boundaries, transgressive surfaces, maximum flooding surfaces, and systems tracts

without referencing sea-level curves or even accommodation curves. Unfortunately the naming of systems tracts (lowstand and highstand) is contaminated by sea-level terms and could be named more correctly lower regressive and upper regressive systems tracts, though we admit that the inertia of the community likely precludes changing these well-worn terms (cf. discussion in Neal and Abreu 2009). Despite this, we conclude that the education of the next generation of sequence stratigraphers be based entirely on objective criteria (as advocated in the initial Exxon Production Research Company approach and reinforced by Neal and Abreu 2009) and we advocate returning "back to basics."

CONCLUSIONS

In contrast to many recent studies that use sea-level curves or accommodation curves to define sequences and systems tracts, we advocate that sequence stratigraphy return to its basic tenets by using objective seismic, core, and well-log criteria to recognize sequence boundaries, transgressive surfaces, maximum flooding surfaces and other flooding surfaces (parasequence boundaries), and systems tracts. We provide Miocene seismic examples from offshore New Jersey that show that continuous coring and logging objectively demonstrate reflection terminations are the physical evidence of sequence boundaries and attendant hiatuses. Cores and logs through these seismic sequences show coarsening and fining-upward packages that provide means for objectively recognizing regressive (LST and HST) and transgressive (TST) systems tracts. These allow the parsing of higher-order depositional sequences within the lower-order (Myr scale) sequences and show that systems tracts interpreted by seismic geometries alone may not fully portray the full stratigraphic hierarchy because of the relatively coarse resolution of the seismic data. Our mid-Cretaceous siliciclastic examples from the New Jersey middle to outer continental shelf apply basic principles to older, commercial seismic profiles and gamma-ray logs to recognize systems tracts and sequences within a biostratigraphic framework. We argue for following the original definition of depositional sequences (Mitchum et al. 1977), although we see little evidence for correlative conformities, and note that some of the names of systems tracts (lowstand and highstand) are contaminated by sea-level terms and should more correctly be thought of and renamed the lower regressive and upper regressive systems tracts, respectively.

SUPPLEMENTAL MATERIAL

Supplemental files are available from JSR's Data Archive: http://sepm.org/pages.aspx?pageid=229.

ACKNOWLEDGMENTS

This work was supported by National Science Foundation grant OCE14-63759 and the Department of Energy under Award Numbers DE-FE0026087 (Mid-Atlantic U.S. Offshore Carbon Storage Resource Assessment Project) and DE-FC26-0NT42589 (Midwest Regional Carbon Sequestration Partnership Program) managed by Battelle. C. Lombardi was supported by the latter before his untimely loss; the work on industry well logs and biostratigraphy was his, and we dedicate this manuscript to his memory. Our work was inspired by the pioneering studies of P. Vail and R. Mitchum, and the suggested topic of "Back to Basics" was provided by J. Neal and V. Abreu. Samples were provided by the International Ocean Discovery Program, and we thank our colleagues on Expedition 313, especially D. Monteverde, who first interpreted the Miocene seismic sequences, for helping foster the ideas presented here. We thank L. Jordan for assistance with biostratigraphic interpretations and P. McLaughlin (Delaware Geological Survey), L. Cummings (Battelle), K. Bohacs, A. Donovan, T.C. Moore, and M. Sullivan for comments on the manuscript.

DISCLAIMER

REFERENCES

Abreu, V., Pederson, K., Neal, J., and Bohacs, K., 2014, A simplified guide for sequence stratigraphy: nomenclature, definitions and method [Abstract]: William Smith Meeting, The Future of Sequence Stratigraphy: Evolution or Revolution? Geological Society of London, 22–23 September 2014.

Ager, D.V., 1973, The Nature of the Stratigraphical Record: New York, John Wiley, 114 p.

Ando, H., Oyama, M., and Nanayama, F., 2014, Data report: grain size distribution of Miocene successions, IODP Expedition 313 Sites M0027, M0028, and M0029, New Jersey shallow shelf, *in* Mountain, G., Proust, J.-N., McInroy, D., Cotterill, C., and the Expedition 313 Scientists, Proceedings of the Integrated Ocean Drilling Program 313: Tokyo, Integrated Ocean Drilling Program Management International, Inc.

Austin, J.A., Christie-Blick, N., Malone, M., and the Leg 174A Shipboard Party, 1998, Proceedings of the Ocean Drilling Program, Initial reports, Volume 174A: College Station, Texas, 324 p.

Bachu, S., 2000, Sequestration of carbon dioxide in geological media: criteria and approach for site selection: Energy Conservation and Management, v. 41, p. 953–970.

Bartek, L.R., Vail, P.R., Anderson, J.B., Emmet, P.A., and Wu, S., 1991, Effect of Cenozoic ice sheet fluctuations in Antarctica on the stratigraphic signature of the Neogene: Journal of Geophysical Research, v. 96, p. 6753–6778.

Brown, L.F., and Fisher, W.L., 1977, Seismic-stratigraphic interpretation of depositional systems: examples from Brazilian rift and pull-apart basins, *in* Payton, C.E., ed., Seismic Stratigraphy: Applications to Hydrocarbon Exploration: American Association of Petroleum Geologists, Memoir 26, p. 213–248.

Browning, J.V., Miller, K.G., Sugarman, P.J., Barron, J., McCarthy, F.M.G., Kulhanek, D.K., Katz, M.E., and Feigenson, M.D., 2013, Chronology of Eocene–Miocene sequences on the New Jersey shallow shelf: implications for regional, interregional, and global correlations: Geosphere, v. 9, p. 1434–1456.

Catuneanu, O., 2002, Sequence stratigraphy of clastic systems: concepts, merits, and pitfalls: Journal of African Earth Sciences, v. 35, p. 1–43.

Catuneanu, O., and 27 others, 2009, Towards the standardization of sequence stratigraphy: Earth-Science Reviews, v. 92, p. 1–33.

Christie-Blick, N., Mountain, G.S., and Miller, K.G., 1990, Seismic stratigraphic record of sea level change, *in* Sea-Level Change: National Academy of Sciences, Studies in Geophysics, National Academy Press, p. 116–140.

Coe, A.L., ed., 2003, The Sedimentary Record of Sea Level Change: Cambridge, UK, Cambridge University Press, 288 p.

Demarest, J.M., and Kraft, J.C., 1987, Stratigraphic record of Quaternary sea levels: implications for more ancient strata, *in* Nummedal, D., Pilkey, O.H., and Howard, J.D., eds., Sea Level Fluctuation and Coastal Evolution: SEPM, Special Publication 41, p. 223–239.

Donovan, A.D., 2010, The sequence stratigraphy family tree: understanding the portfolio of sequence methodologies, *in* Ratcliffe, K., and Zaitlin, B.A., eds., Application of Modern Stratigraphic Techniques: Theory and Case Histories: SEPM, Special Publication 94, p. 5–53.

Eberli, G.E., Anselmetti, F.S., Kroon, D., Sato, T., and Wright, J.D., 2002, The chronostratigraphic significance of seismic reflections along the Bahamas Transect: Marine Geology, v. 185, p. 1–17.

Embry, A., 2009, Practical Sequence Stratigraphy: Canadian Society of Petroleum Geologists: Online at www.cspg.org, 81 p.

Embry, A.F., Johannessen, E.P., 1992, T–R sequence stratigraphy, facies analysis and reservoir distribution in the uppermost Triassic–Lower Jurassic succession, western Sverdrup basin, Arctic Canada, *in* Vorren, T.O., Bergsager, E., Dahl-Stamnes, O.A., Holter, E., Johansen, B., Lie, E., and Lund, T.B. eds., Arctic Geology and Petroleum Potential: Norwegian Petroleum Society, Special Publication, v. 2, p. 121–146.

Emery, K.O., 1968, Positions of empty pelecypod valves on the continental shelf: Journal of Sedimentary Petrology, v. 38, p. 1264–1269.

Galloway, W.E., 1989, Genetic stratigraphic sequences in basin analysis I: architecture and genesis of flooding surface bounded depositional units: American Association of Petroleum Geologists, Bulletin, v. 73, p. 125–142.

Goff, J.A., Austin, J.A., Jr., and Fulthorpe, C.S., 2013, Reinterpretation of the Franklin "Shore" in the Mid-Atlantic bight as a paleo-shelf edge: Continental Shelf Research, v. 60, p. 64–69.

Gradstein, F.M., Ogg, J.G., Schmitz, M., and Ogg, G., 2012, The Geologic Time Scale 2012: Oxford, UK, Elsevier, v. 1–2, 1176 p.

Greenlee, S.M., Devlin, W.J., Miller, K.G., Mountain, G.S., and Flemings, P.B., 1992, Integrated sequence stratigraphy of Neogene deposits, New Jersey continental shelf and slope: comparison with the Exxon model: Geological Society of America, Bulletin, v. 104, p. 1403–1411.

Grow, J.A., and Sheridan, R.E. 1988, U.S. Atlantic continental margin: a typical Atlantic-type or passive continental margin, *in* Sheridan, R.E., and Grow, J.A., eds., The Atlantic Continental Margin: Boulder, Colorado, Geological Society of America, Geology of North America, v. 1–2, p. 1–7.

Haq, B.U., 2014, Cretaceous eustasy revisited: Global and Planetary Change, v. 113, p. 44–58.

Haq, B.U., Hardenbol, J., and Vail, P.R., 1987, Chronology of fluctuating sea levels since the Triassic (250 million years ago to present): Science, v. 235, p. 1156–1167.

Heezen, B.C., Tharp, M., and Ewing, M., 1959, The Floors of the Oceans: Geological Society of America, Special Paper 65, 122 p.

Hlavaty, C.L., Kopp, R.E., Miller, K.G., Browning, J.V., Reinfelder, Y.F., Mountain, G.S., and Slater, B., 2012, Carbon sequestration beneath the New Jersey continental shelf: an assessment of the geological and socio-political factors [Abstract]: Geological Society of America, Abstracts with Programs, v. 44, p. 239.

Hunt, D., and Tucker, M.E., 1992, Stranded parasequences and the forced regressive wedge systems tract: deposition during base level fall: Sedimentary Geology v. 81, p. 1–9.

Jansa, L.F., 1981, Mesozoic carbonate platforms and banks of the eastern North American margin: Marine Geology, v. 44, p. 97–117.

Karlos, J.F., 1986, Results of exploration in the Mesozoic shelf-edge carbonates, Baltimore Canyon Basin [Abstract]: American Association of Petroleum Geologists, Bulletin, v. 70, p. 605–606.

Katz, M.E., Browning, J.V., Miller, K.G., Monteverde, D., Mountain, G.S., and Williams, R.H., 2013, Paleobathymetry and sequence stratigraphic interpretations from benthic foraminifera: insights on New Jersey shelf architecture, IODP Expedition 313: Geosphere, v. 9, p. 1488–1513.

Kidwell, S.M., 1989, Stratigraphic condensation of marine transgressive records: origin of major shell deposits in the Miocene of Maryland: Journal of Geology, v. 97, p. 1–24.

Kidwell, S.M., 1991, The stratigraphy of shell concentration, *in* Allison, P.A., and Briggs, D.E.G., eds., Taphonomy: Releasing the Data Locked in the Fossil Record: New York, Springer-Verlag, Topics in Geobiology, v. 9, p. 211–290.

Kominz, M.A., Miller, K.G., and Browning, J.V., 1998, Long-term and short-term global Cenozoic sea-level estimates: Geology, v. 26, p. 311–314.

Kominz, M.A., Van Sickel, W.A., Miller, K.G., and Browning, J.V., 2002, Sea-level estimates for the latest 100 million years: one-dimensional backstripping of onshore New Jersey boreholes, *in* Armentrout, J., and Rosen, N., eds., Sequence Stratigraphic Models for Exploration and Production: Evolving Methodology, Emerging Models and Application Case Histories: 22nd Annual Gulf Coast Section, SEPM Foundation, Bob F. Perkins Research Conference, Proceedings, p. 303–315.

Libby-French, J., 1984, Stratigraphic framework and petroleum potential of northeastern Baltimore Canyon Trough, mid-Atlantic outer continental shelf: American Association of Petroleum Geologists, Bulletin, v. 68, p. 50–73.

Lippert, R.H., 1983, The "Great Stone Dome": a compaction structure, *in* Bally, A.W., ed., Seismic Expression of Structural Styles: A Picture and Work Atlas, Volume 1, The Layered Earth: American Association of Petroleum Geologists, Studies in Geology 15, p. 1.3–1.

Litynski, J.T., Brown, B.M., Vikara, D.M., and Srivastava, R.D., 2011, Carbon capture and sequestration: the U.S. Department of Energy's R&D efforts to characterize opportunities for deep geologic storage of carbon dioxide in offshore resources OTC-21987-PP, presented at the Houston Offshore Technology Conference, Proceedings.

Loutit, T.S., Hardenbol, J., Vail, P.R., and Baum, G.R., 1988, Condensed section: the key to age determination and correlation of continental margin sequences, *in* Wilgus, C.K., Hastings, B.S., Kendall, C.G.St.C., Posamentier, H.W., Ross, C.A., and Van Wagoner, J.C., eds., Sea Level Changes: An Integrated Approach: SEPM, Special Publication 42, p. 183–213.

Metz, B., Davidson, O., de Coninck, H., Loos, M., and Meyer, L., 2005, IPCC Special Report on Carbon Dioxide Capture and Storage: Cambridge University Press, New York, 443 p., https://www.ipcc.ch/pdf/special-reports/srccs/srccs_wholereport.pdf.

Miller, K.G., and Mountain, G.S., 1994, Global sea-level change and the New Jersey margin, *in* Mountain, G.S., Miller, K.G., Blum, P., et al., Proceedings of the Ocean Drilling Program, Initial reports, Volume 150: College Station, Texas, p. 11–20.

Miller, K.G., Mountain, G.S., the Leg 150 Shipboard Party, and Members of the New Jersey Coastal Plain Drilling Project, 1996, Drilling and dating New Jersey Oligocene–Miocene sequences: ice volume, global sea level, and Exxon records: Science, v. 271, p. 1092–1094.

Miller, K.G., Mountain, G.S, Browning, J.V., Kominz, M., Sugarman, P.J., Christie-Blick, N., Katz, M.E., and Wright, J.D., 1998, Cenozoic global sea-level, sequences, and the New Jersey transect: results from coastal plain and slope drilling: Reviews of Geophysics, v. 36, p. 569–601.

Miller, K.G., Sugarman, P.J., and Browning, J.V., 2001, Ocean View Site, *in* Miller, K.G., Sugarman, P.J., Browning, J.V., et al., eds., Proceedings of the Ocean Drilling Program, Initial reports, Volume 174AX (Suppl.): College Station, Texas, p. 1–72.

Miller, K.G., Kominz, M.A., Browning, J.V., Wright, J.D., Mountain, G.S., Katz, M.E., Sugarman, P.J., Cramer, B.S., Christie-Blick, N., and Pekar, S.F., 2005, The Phanerozoic record of global sea-level change: Science, v. 310, p. 1293–1298.

Miller, K.G., Browning, J.V., Mountain, G.S., Bassetti, M.A., Monteverde, D., Katz, M.E., Inwood, J., Lofi, J., and Proust, J.-N., 2013a, Sequence boundaries are impedance contrasts: core–seismic–log integration of Oligocene–Miocene sequences, New Jersey shallow shelf: Geosphere, v. 9, p. 1257–1285.

Miller, K.G., Mountain, G.S., Browning, J.V., Katz, M.E., Monteverde, D.H., Sugarman, P.J., Ando, H., Bassetti, M.A., Bjerrum, C.J., Hodgson, D., Hesselbo, S., Karakaya, S., Proust, J.-N., and Rabineau, M., 2013b, Testing sequence stratigraphic models by drilling Miocene foresets on the New Jersey shallow shelf: Geosphere, v. 9, p. 1236–1256.

Miller, K.G., Browning, J.V., Mountain, G.S., Sheridan, R.E., Sugarman, P.J., Glenn, S., and Christensen, B.A., 2014, History of continental shelf and slope sedimentation on the U.S. Middle Atlantic margin, *in* Chiocci, F.L., and Chivas, A.R., eds., Continental Shelves of the World: Their Evolution During the Last Glacio-Eustatic Cycle: Geological Society of London, Special Publication 41, p. 21–34.

Miller, K.G., Baluyot, R., Wright, J.D., Kopp, R.E., and Browning, J.V., 2017, Closing an early Miocene astronomical gap with Southern Ocean $\delta^{18}O$ and $\delta^{13}C$ records: implications for sea-level change: Paleoceanography, v. 32, doi:10.1002/ 2016PA003074.

Mitchum, R.M., Jr., 1977, Seismic stratigraphy and global changes of sea level: Part 11. Glossary of terms used in seismic stratigraphy: Section 2. Application of seismic reflection configuration to stratigraphic interpretation, *in* Payton, C.E., ed., Seismic Stratigraphy: Applications to Hydrocarbon Exploration: American Association of Petroleum Geologists, Memoir 26, p. 205–212.

Mitchum, R.M., Jr., and Van Wagoner, J.C., 1991, High-frequency sequences and their stacking patterns: sequence-stratigraphic evidence of high-frequency eustatic cycles: Sedimentary Geology, v. 70, p. 131–160.

Mitchum, R.M., Jr., Vail, P.R., Thompson, S., III, 1977, Seismic stratigraphy and global changes of sea level; Part 2, The depositional sequence as a basic unit for stratigraphic analysis, *in* Payton, C.E., ed., Seismic Stratigraphy: Applications to Hydrocarbon Exploration: American Association of Petroleum Geologists, Memoir 26, p. 53–62.

Mitrovica, J.X., 2009, Eulogy for eustasy [Abstract]: American Geophysical Union, EOS Transactions, v. 90, Fall Meeting Birch Lecture, Abstract T34A.

Monteverde, D.H., 2008, Sequence stratigraphic analysis of early and middle Miocene shelf progradation along the New Jersey margin [Ph.D. thesis]: New Brunswick, Rutgers University, 247 p.

Monteverde, D.H., Mountain, G.S., Miller, K.G., 2008, Early Miocene sequence development across the New Jersey margin: Basin Research, v. 20, p. 249–267.

Moucha, R., Forte, A.M., Mitrovica, J.X., Rowley, D.B., Quere, S., Simmons, N.A., and Grand, S.P., 2008, Dynamic topography and long-term sea level variations: there is no such thing as a stable continental platform: Earth and Planetary Science Letters, v. 271, p. 101–108.

Mountain, G., and Monteverde, D., 2012, If you've got the time, we've got the depth: the importance of accurate core–seismic correlation [Abstract]: American Geophysical, Union Fall Meeting, abstract PP51B–2111.

Mountain, G.S., Miller, K.G., and Blum, P., 1994, Proceedings of the Ocean Drilling Program, Initial Reports, Volume 150, 885 p.

Mountain, G., Damuth, J.E., McHugh, C.M.G., Lorenzo, J., and Fulthorpe, C., 1996, Origin, reburial and significance of a mid-Miocene canyon, New Jersey continental slope, *in* Mountain, G.S., Miller, K.G., Blum, P., and Twitchell, D.C., et al., Proceedings of the Ocean Drilling Program, Scientific Results, Volume 150: College Station, Texas, p. 283–292.

Mountain, G.S., Burger, R.L., Delius, H., Fulthorpe, C.S., Austin, J.A., Goldberg, D.S., Steckler, M.S., McHugh, C.M., Miller, K.G., Monteverde, D.H., Orange, D.L., and Pratson, L.F., 2007, The long-term stratigraphic record on continental margins, *in* Nittrouer, C.A., Austin, J.A., Jr., Field, M.E., Kravitz, J.H., Syvitski, J.M., and Wiberg, L., eds., Continental-Margin Sedimentation: From Sediment Transport To Sequence Stratigraphy: International Association of Sedimentologists, Special Publication 37, p. 381–45.

Mountain, G.S., Proust, J.-N., McInroy, D., Cotterill, C., and the Expedition 313 Scientists, 2010, Initial Report: Proceedings of the International Ocean Drilling Program, Expedition 313, College Station, Texas.

Neal, J., and Abreu, V., 2009, Sequence stratigraphy hierarchy and the accommodation succession method: Geology, v. 37, p. 779–782.

Nystuen, J.P., 1998, History and development of sequence stratigraphy, *in* Gradstein, F.M., Sandvik, K.O., and Milton, N.J., eds., Sequence Stratigraphy: Concepts and Applications: Norwegian Petroleum Society, Special Publication 8, p. 31–116.

Olsson, R.K., Melillo, A.J., and Schreiber, B.L., 1987, Miocene sea level events in the Maryland coastal plain and the offshore Baltimore Canyon trough, *in* Ross, C., and Haman, D., eds., Timing and Depositional History of Eustatic Sequences: Constraints on Seismic Stratigraphy: Cushman Foundation for Foraminiferal Research, Special Publication 24, p. 85–97.

Olsson, R.K., Gibson, T.G., Hansen, H.J., and Owens, J.P., 1988, Geology of the northern Atlantic coastal plain: Long Island to Virginia, *in* Sheridan, R.E., and Grow, J.A., eds.,

The Atlantic Continental Margin: Geological Society of America, Geology of North America, v. 1–2, p. 87–105.

Peltier, W.R., 1998, Postglacial variations in the level of the sea: implications for climate dynamics and solid-Earth geophysics: Reviews of Geophysics, v. 36, p. 603–689.

Pitman, W.C., III, and Golovchenko, X., 1983, The effect of sea-level change on the shelf edge and slope of passive margins, *in* Stanley, D.J., and Moore, G.T., eds., The Shelfbreak: Critical Interface on Continental Margins: SEPM, Special Publication 33, p. 41–58.

Plint, A.G., and Nummedal, D., 2000, The falling stage systems tract: recognition and importance in sequence stratigraphic analysis, *in* Hunt, D., and Gawthorpe, R.L., eds., Sedimentary Response to Forced Regression: Geological Society of London, Special Publication 172, p. 1–17.

Posamentier, H.W., and Allen, G.P., 1999, Siliciclastic Sequence Stratigraphy: Concepts and Applications: SEPM, Concepts in Sedimentology and Paleontology 7, 210 p.

Posamentier, H.W., and Vail, P.R., 1988, Eustatic controls on clastic deposition II: sequence and systems tract models, *in* Wilgus, C.K., Hastings, B.S., Kendall, C.G.St.C., Posamentier, H.W., Ross, C.A., and Van Wagoner, J.C., eds., Sea Level Changes: An Integrated Approach: SEPM, Special Publication 42, p. 125–154.

Posamentier, H.W., Jervey, M.T., and Vail, P.R., 1988, Eustatic controls on clastic deposition I: conceptual framework, *in* Wilgus, C.K., Hastings, B.S., Kendall, C.G.St.C., Posamentier, H.W., Ross, C.A., and Van Wagoner, J.C., eds., Sea Level Changes: An Integrated Approach: SEPM, Special Publication 42, p. 109–124.

Posamentier, H.W., Allen, G.P., James, D.P., and Tesson, M., 1992, Forced regressions in a sequence stratigraphic framework: concepts, examples, and exploration significance: American Association of Petroleum Geologists, Bulletin, v. 76, p. 1687–1709.

Prather, B.E., 1991, Petroleum geology of the Upper Jurassic and Lower Cretaceous, Baltimore Canyon Trough, western North Atlantic Ocean: American Association of Petroleum Geologists, Bulletin, v. 75, p. 258–277.

Pratson, L.F., Ryan, W.B.F., Mountain, G.S., and Twichell, D.C., 1994, Submarine canyon initiation by downslope-eroding sediment flows: evidence in late Cenozoic strata on the New Jersey continental slope: Geological Society of America, Bulletin, v. 106, p. 395–412.

Proust, J.N., Mahieux, G., and Tessier, B., 2001, Field and seismic images of sharp-based shoreface deposits: implications for sequence stratigraphic analysis: Journal of Sedimentary Research, v. 71, p. 944–957.

Rabineau, M., Berné, S., Aslanian, D., Olivet, J.-L., Joseph, P., Guillocheau, F., Bourillet, J.-F., Ledrezen, E., and Granjeon, D., 2005, Sedimentary sequences in the Gulf of Lions: a record of 100,000 years climatic cycles: Marine and Petroleum Geology, v. 22, p. 775–804.

Raymo, M.E., Mitrovica, J.X., O'Leary, M.J., DeConto, R.M., and Hearty, P.J., 2011, Departures from eustasy in Pliocene sea-level records: Nature Geoscience, v. 4, p. 328–332.

Rowley, D.B., Forte, A.M., Moucha, R.R., Mitrovica, J.X., Simmons, N.A., and Grand, S.P., 2011, Dynamic topography change of the eastern U.S. since 4 Ma: implications for sea level and stratigraphic architecture of passive margins: Science, v. 340, p. 1563–1563.

Scholle, A., 1977, Data summary and petroleum potential, *in* Scholle, A., ed., Geological Studies on the COST No. B-2 Well, U.S. Mid-Atlantic Outer Continental Shelf Area: U.S. Geological Survey, Circular 750, p. 8–14.

Scholle, P.A., 1980, Cost No. B-2 well, *in* Mattick, R.E., and Hennessy, J.L., eds., Structural Framework, Stratigraphy and Petroleum Geology of the Area of Oil and Gas Lease Sale No. 49 on the U.S Atlantic Continental Shelf and Slope: U.S. Geological Survey, Circular 812, p. 79–84.

Seker, Z., 2012, Cretaceous well-log and sequence stratigraphic correlation of the outer continental shelf and upper slope off of New Jersey [M.S. thesis]: Rutgers University, 155 p.

Steckler, M.S., and Watts, A.B., 1978, Subsidence of the Atlantic-type continental margins off New York: Earth and Planetary Science Letters, v. 41, p. 1–13.

Steckler, M.S., Mountain, G.S., Miller, K.G., and Christie-Blick, N., 1999, Reconstruction of Tertiary progradation and clinoform development on the New Jersey passive margin by 2-D backstripping: Marine Geology, v. 154, p. 399–420.

Talwani, M., Ewing, J., Sheridan, R.E., Holbrook, W.S., and Glover, L., III, 1995, The EDGE experiment and the U.S. East Coast magnetic anomaly, *in* Banda, E., Torne, M., and Talwani, M., eds., Rifted Ocean–Continent Boundaries: Dordrecht, Kluwer Academic Publishers, p. 155–181.

Trincardi, F., and Correggiari, A., 2000, Quaternary forced regression deposits in the Adriatic Basin and the record of composite sea-level cycles, *in* Hunt, D., and Gawthorpe, R., eds., Sedimentary Responses to Forced Regressions: Geological Society of London, Special Publication 172, p. 245–269.

Vail, P.R., 1987, Seismic stratigraphy interpretation using sequence stratigraphy, Part 1: seismic stratigraphy interpretation procedure, *in* Bally, A.W., ed., Atlas of Seismic Stratigraphy: American Association of Petroleum Geologists, Studies in Geology 27, p. 1–10.

Vail, P.R., and Todd, R.G., 1981, Northern North Sea Jurassic unconformities, chronostratigraphy, and sea-level changes from seismic stratigraphy, *in* Illing, L.V., and Hobson, G.O., eds., Petroleum Geology of the Continental Shelf of Northwest Europe: London, Institute of Petroleum, p. 216–235.

Vail, P.R., Mitchum, R.M., Jr., and Thompson, S., III., 1977, Seismic stratigraphy and global changes of sea level, Part 4: global cycles of relative changes of sea level, *in* Payton, C.E., ed., Seismic Stratigraphy: Applications to Hydrocarbon Exploration: American Association of Petroleum Geologists, Memoir 26, p. 83–97.

Van Noorden, R., 2010, Carbon sequestration: buried trouble: Nature, v. 463, p. 871–873.

Van Wagoner, J.C., Mitchum, R.M., Jr., Posamentier, H.W., and Vail, P.R., 1987, Seismic stratigraphy interpretation using sequence stratigraphy: Part 2, Key definitions of sequence stratigraphy, *in* Bally, A.W., ed., Atlas of Seismic Stratigraphy: American Association of Petroleum Geologists, Studies in Geology 27, p. 11–14.

Van Wagoner, J.C., Posamentier, H.W., Mitchum, R.M., Vail, P.R., Sarg, J.F., Loutit, T.S., and Hardenbol, J., 1988, An overview of the fundamentals of sequence stratigraphy and key definitions, *in* Wilgus, C.K., Hastings, B.S., Kendall, C.G.St.C., Posamentier, H.W., Ross, C.A., and Van Wagoner, J.C., eds., Sea Level Changes: An Integrated Approach: SEPM, Special Publication 42, p. 39–45.

Van Wagoner, J.C., Mitchum, R.M., Campion, K.M., and Rahmanian, V.D., 1990, Siliciclastic sequence stratigraphy in well logs, cores, and outcrops: concepts for high-resolution correlation of time and facies: American Association of Petroleum Geologists, Methods in Exploration Series 7, 55 p.

Watts, A.B., 1981, The U.S. Atlantic continental margin: subsidence history, crustal structure, and thermal evolution, *in* Bally, A.W., ed., Geology of Passive Continental Margins: History, Structure, and Sedimentologic Record: American Association of Petroleum Geologists, Education Course Note Series 19, p. 2-i-2–70.

Wheeler, H.E., 1958, Time stratigraphy: American Association of Petroleum Geologists, Bulletin, v. 42, p. 1047–1063.

Withjack, M.O., Schlische, R.W., and Olsen, P.E., 1998, Diachronous rifting, drifting, and inversion on the passive margin of central eastern North America: an analog for other passive margins: American Association of Petroleum Geologists, Bulletin, v. 82, p. 817–835.

Zoback, M.D., and Gorelick, S.M., 2012, Earthquake triggering and large-scale geologic storage of carbon dioxide: National Academy of Sciences, Proceedings, v. 109, p. 10164–10168.

Received 12 April 2017; accepted 21 October 2017.